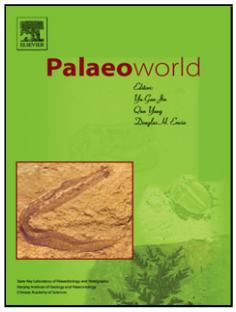

Title: New fossils of *Eucladoceros boulei* (Artiodactyla, Mammalia) from Early Pleistocene Nihewan Beds, China

Authors: Hao-Wen Tong, Bei Zhang

PII: S1871-174X(19)30004-6
DOI: https://doi.org/10.1016/j.palwor.2019.05.003
Reference: PALWOR 506

To appear in: *Palaeoworld*

Received date: 15 January 2019
Revised date: 13 March 2019
Accepted date: 14 May 2019

Please cite this article as: Tong H-Wen, Zhang B, New fossils of *Eucladoceros boulei* (Artiodactyla, Mammalia) from Early Pleistocene Nihewan Beds, China, *Palaeoworld* (2019), https://doi.org/10.1016/j.palwor.2019.05.003

New fossils of *Eucladoceros boulei* (Artiodactyla, Mammalia) from Early Pleistocene Nihewan Beds, China

Hao-Wen Tong [a, b] *, Bei Zhang [a, b, c]

[a] Key Laboratory of Vertebrate Evolution and Human Origins of Chinese Academy of Sciences, Institute of Vertebrate Paleontology and Paleoanthropology, Chinese Academy of Sciences, Beijing 100044, China

[b] CAS Center for Excellence in Life and Paleoenvironment, Beijing 100044, China

[c] University of Chinese Academy of Sciences, Beijing 100049, China

* Corresponding author. *E-mail address*: tonghaowen@ivpp.ac.cn

Abstract

Recent excavations at Shanshenmiaozui site in Nihewan Basin of North China uncovered a rich collection of comb-antlered deer, which includes the first discovery of the yearling antler, complete upper and lower dentitions (both deciduous and permanent), associated limb bones including the longest metapodials ever recovered. Based on toothrow length and the dental characters as well as the postcranial bones, the new fossil materials can be referred to *Eucladoceros boulei* that is estimated to be 350 kg and represents the largest Pleistocene cervid ever recovered in China. Besides the large size, *E. boulei* is also characterized by the pronounced anterior cingulids and entostylid ribs on lower molars as well as the moderately pachyostosed mandibles. The present study shows that the body weight of large cervids can be estimated by the length of toothrow and metacarpal, with exception for *Cervus elaphus*, which has larger toothrow length, but shorter metacarpal and smaller body size. *E. boulei* is a typical element of the Early Pleistocene fauna in northern China. The early Villafranchian is a bottleneck period for cervid evolution in northern China, which is characterized by the following features: decrease of cervid diversity, disappearance of archaic groups, and the rise of the medium to large-sized three-tined cervini taxa. The sudden appearance of the very large and/or multi-tined cervids at the Pliocene–Pleistocene transition may represent a great migration event of mammals. The Early Pleistocene cervids from Nihewan Basin

are very diverse, and are in need of more taxonomic work.

Keywords: *Eucladoceros*; Early Pleistocene; Shanshenmiaozui; Nihewan; China

1. Introduction

The Nihewan Fauna is dominated by canids and ungulates, among which cervid is also important in inter-regional correlation and in evolutionary studies as well as in paleoenvironmental reconstructions. Four cervid taxa, though insufficiently studied, were first identified in the Nihewan Fauna, namely *Cervulus* cf. *sinensis*, *Cervus* (*Eucladoceros*) *boulei*, *Cervus* (*Elaphurus*) *bifurcatus*, and *Cervus* (*Rusa*) *elegans* (Teilhard de Chardin and Piveteau, 1930). They were later revised as follows: *Muntiacus* (= *Cervulus*) *bohlini*, *Eucladoceros boulei*, *Elaphurus bifurcatus*, and *Pseudodama elegans* (Teilhard de Chardin and Leroy, 1942; Qiu, 2000). Among these, *E. boulei* is the most common species and best represented by crania, antlers, dental and postcranial elements.

E. boulei is the most peculiar species in the comb-antlered deer (genus *Eucladoceros*), which is quite different from its European kins and would never be confused with other co-generic species (Heintz, 1970; Azzaroli and Mazza, 1992a; van der Made, 2015). *Eucladoceros* species are recorded from Late Pliocene to latest Early Pleistocene (Azzaroli and Mazza, 1992a), and are regarded as the characteristic taxa of the Nihewanian mammal age in northern China (Woodburne et al., 2013), which means this group is very important both in evolutionary and chronological studies. However, the crucial questions about the morphological, phylogenetic and chronological positions as well as the migrations of *Eucladoceros* remain unresolved in China; especially the postcranial bones of *E. boulei* are virtually undescribed in the literature (Azzaroli and Mazza, 1992a). During the past decade, more specimens of *E. boulei* were unearthed from the newly recovered Shanshenmiaozui site in Nihewan Basin, including, maxillae and mandibles with teeth attached in situ, antlers and postcranial bones, some of which were preserved in articulated position. These fossils are significant for the further studies on the paleontological issues for *E. boulei*.

The Shanshenmiaozui fossil site (40º13’08”N, 114º39’54”E) is located at the southern bank of the Sangganhe River, at the edge of Haojiatai fluvio-lacustrine platform in Yangyuan County, Hebei Province (Fig. 1). Based on the stratigraphic correlation, the fossil-bearing sand-silt bed at the new site is slightly higher than the

Paleolithic layer at Xiaochangliang site (Tong et al., 2011; Liu et al., 2016). The paleomagnetic age of the latter is about 1.36 Ma (Zhu et al., 2001); while the former is ca. 1.2 Ma (Liu et al., 2016), even though the mammalian fossil assemblage seems to indicate a biochronological age older than 1.2 Ma.

The mammalian taxa associated with *E. boulei* at the Shanshenmiaozui site include: *Lepus* sp., *Ochotona* sp., *Canis chihliensis*, Pantherinae gen. et sp. indet., *Pachycrocuta* sp., *Mammuthus trogontherii*, *Coelodonta nihowanensis*, *Elasmotherium peii*, *Proboscidipparion* sp., *Equus sanmeniensis*, *Sus* sp., *Spirocerus wongi*, *Bison palaeosinensis*, and *Gazella sinensis* (Tong et al., 2011, 2017; Tong, 2012; Tong and Wang, 2014; Tong and Chen, 2015). The field work between 2015 and 2018 recovered some more taxa, e.g., *Alactaga* sp. (represented by a metacarpal bone), *Acinonyx* sp. (radius), *Panthera* sp. (partial mandible and manus bones), *Lynx* sp. (partial mandible with m1), *Paracamelus* sp. (partial metatarsal), *Nipponicervus* cf. *elegans* (partial antler and metacarpal) and *Gazella subgutturosa* (metatarsal).

2. Materials and methods

All of the fossils of *E. boulei* studied in this paper were recently recovered from the Shanshenmiaozui Locality (Table S1 in Supplementary data). All the specimens described in this paper are deposited in the collection of IVPP in Beijing.

The classification system is after Azzaroli and Mazza (1992a), Sheng (1992), de Vos et al. (1995), Grubb (2000), Groves and Grubb (2011). The biochronological system follows Tong et al. (1995), Qiu (2000, 2006), and Zhu et al. (2007).

Antler terminology is after Putman (1988) and Bubenik (1990). The dental terminology (Fig. 2) is after Gentry (1994), Lister (1996), Dong (2004), Bärmann and Rössner (2011), Vislobokova (2012), Gustafson (2015), van der Made (2015), and Suraprasit et al. (2016).

The osteological terms are after Brown and Gustafson (1979), Lister (1996), Breda (2005), and Senter and Moch (2015). The dental age estimation is after Brown (1991). The phenotypic characters evaluation is after O'Leary and Gatesy (2008). The upper and lower teeth were denoted by uppercase and lowercase letters respectively. The postcranial bones were identified according to the method employed by Brown and Gustafson (1979), Prummel (1988). The specimens were measured according to the methods used by von den Driesch (1976), van der Made and Tong (2008) and van der Made (2015). The linear measurements were taken with sliding caliper in

millimeters. The cross-section images of the antler and mandibles were obtained by CT scanning.

The body mass estimation is after the methods by Scott (1983, 1990), Damuth and MacFadden (1990). The size classes of the body mass are after Brugal and Croitor (2007): small: < 20 kg; medium: 20–100 kg; large: 100–300 kg; very large: > 300 kg.

Institution and locality abbreviations: BMNH, Beijing Museum of Natural History; **HPICR**, Hebei Province Institute of Cultural Relics; **IOZ**, Institute of Zoology, Beijing; **IVPP**, Institute of Vertebrate Paleontology and Paleoanthropology; **MNHN**, Muséum National d'Histoire Naturelle; **NM**, Nihewan Museum; **NNNRM**, Nihewan National Nature Reserve Management; **OV**, Prefix to the Catalogue numbers of extant specimens in IVPP; **SSMZ**, Shanshenmiaozui; **TNHM**, Tianjin Natural History Museum; **V**, Prefix in the catalog numbers for vertebrate fossils in IVPP; **XSG**, Xiashagou; **YS**, Yushe. **E. Pleis**, Early Pleistocene; **M. Pleis**, Middle Pleistocene; **L. Pleis**, Late Pleistocene.

Morphological abbreviations: DAP, anteroposterior diameter; **DT**, transverse diameter; **Mc**, metacarpal; **Mt**, metatarsal; **Mc III+IV**, metacarpal III+IV; **Mt III+IV**, metatarsal III+IV; **PI**, Pachyostosis Index.

3. Systematic paleontology

3.1. Classifications

Class Mammalia Linnaeus, 1758
Order Artiodactyla Owen, 1848
Suborder Ruminantia Scopoli, 1777
Infraorder Pecora Linnaeus, 1758
Superfamily Cervoidea Goldfuss, 1820
Family Cervidae Goldfuss, 1820
Subfamily Cervinae Goldfuss, 1820

Genus *Eucladoceros* Falconer, 1868

1898 *Euctenoceros* – Trouessart, p. 880.

Type species: *Eucladoceros dicranios* (Nesti, 1841).

Generic diagnosis: Large-sized deer of plesiometacarpal form; antler with 4 to 6 prongs normally, and with all the tines direct forward and comb-like, in some cases the tines are further branched. The dentition is generally primitive, and with pillars at the outlets of the valleys between crescents in the upper molars; in the lower molars, these pillars decrease in size from m1 to m3; p4 is generally simple and with lower degree of molarization; the lower premolar series is relatively long compared to molars (Teilhard de Chardin and Piveteau, 1930; Heintz, 1970; Azzaroli and Mazza, 1992a; Croitor, 2017).

Eucladoceros boulei (Teilhard de Chardin and Piveteau, 1930)
(Figs. 1-8)

1930 *Cervus* (*Eucladoceros*) *boulei* – Teilhard de Chardin and Piveteau, p. 48, text-figs. 18-19, pls. 8-10.
1935 *Cervus* cf. *boulei* – Young, p. 10, text-fig. 3.
1965 *Euctenoceros* sp. – Chow and Chow, p. 226, pl. 2, figs. 1, 2.
1978 *Euctenoceros boulei* – Chia and Wang, p. 19, pl. 8.
1980 *Euctenoceros boulei* – Tang, p. 39, pl. 2, fig. 6.
1983 *Euctenoceros* sp. – Tang et al., p. 81.
1985 cf. *Euctenoceros* sp. – Zheng et al., p. 127, pl. 6, fig. 2.

Emended diagnosis (osteo-dental) (modified from Teilhard de Chardin and Piveteau, 1930): Antler with a long shaft (i.e., high bifurcation between brow tine and main beam) which has a circular cross-section; each antler with 4 to 6 prongs, all the tines direct forward and the whole antler looks comb-like except the partial coalescence of the crown tines in some cases, and the antler crown is flattened both for beam and tines. Skull with large and deep preorbital fossae; orbits are prominently protruding and moderately tubular shaped. Mandible is moderately pachyostosed. Upper premolars only have weak inner wall split, which is completely disappeared in P4; upper molars have weak anterior cingulum; lower p3 and p4 have their posterior valleys closed, but the anterior valleys are usually open; lower molars have pronounced anterior cingulid and entostylid ribs. Metapodials are long but gracile.
Locality: Shanshenmiaozui, Yangyuan County, Hebei Province, China.
Horizon: Early Pleistocene, older than 1.2 Ma.

3.2. Descriptions

3.2.1. Antlers

The two partial antlers (IVPP V 25966.1 and IVPP V 25966.2) were identified as juvenile or the first-year (yearling) antlers as they bear such characteristics of the first antlers in yearlings like generally bare knobs, small, unbranched spikes or forklettes without burrs (Bubenik, 1990). Although they were not recovered together, they should be a pair according to their sizes and orientations as well as development stage. The specimen IVPP V 25966.1 still has partial frontal bone attached. The features of these yearling antlers are unbranched, burr-less, but they are not so small in diameter and length as in other taxa, especially the pedicle is quite long and robust, and has obviously larger diameter than the yearling antler. The surface of the spike is full of longitudinal grooves and with few small tubercles, but not so rugose as in *Axis shansius*, and is fully mineralized (Fig. 3A, B). The CT scanning can detect the internal structure change at the tip of the pedicle (Fig. 3C), where the bone structure is very porous (the bright white part in photo of Fig. 3C) and saucer-like, which represents the boundary between the antler and the pedicle according to the study for extant deer antler (Kierdorf et al., 2013). There is no distinct boundary between the spike and the pedicle (i.e., absence of burr); but the close up of the pedicle to antler transition can demonstrate the nodose ornamentation in the position of the future burr in *Cervus* (*Rusa*) *unicolor* (Heckeberg, 2017, fig. 2.9).

Although the first-year antlers of most living cervids vary considerably in size and shape depending on a combination of heredity, health, and nutrition (Gustafson, 2015); in red deer, yearling antler length varies from a minimum of 1.4 cm (1985 cohort) to a maximum of 12.9 cm (1970 cohort) (Schmidt et al., 2001); in moose (*Alces alces*), the maximum shaft circumferences of the antlers generally increase from 1.5–13.5 years and decrease thereafter (Child et al., 2010). The study on the pedicles of extant red deer shows that the length decreases with age, whereas the diameter increases with age (Degmečić et al., 2013), which can explain the different dimensions of juvenile and adult *E. boulei* antlers (Table S2 in Supplementary data).

The SSMZ specimens are among the largest spikes of all cervids ever reported in China, and represent the first recovery of the yearling antlers for its species and even for its genus.

3.2.2. Jaw bones

3.2.2.1. Maxillaries

More than 6 partial maxillaries have been recovered (Figs. 4-6), most of them with toothrows preserved in alveoli. The maxillaries, either juvenile or adult, have no specialty. The only character observable is the infraorbital foramen, which is located above the paracone of DP2 or P2. The facial tubercle is not prominent.

3.2.2.2. Mandibles

The new collection contains 12 mandibles (Figs. 4-6; Table S3 in Supplementary data); most of them are juvenile, with complete deciduous or permanent dentitions. All the mandibles show the following features: mandibles with obvious pachyostosis (Fig. 5D); the coronoid process is quite robust; the mandibular notch is narrow and deep; the depth of the horizontal ramus is reduced sharply in front of p2, and the profile of the inferior border of the mandible is convex, and the muzzle part ascends sharply from the point corresponding with p4; the superior edge at the diastema part is not so sharpened as in sika deer; there are two mental foramens, the much bigger one corresponds with the rear edge of the symphysis which is more prominently posterior than in sika deer, and the tiny one is just under dp2 or p2; the angular process is not clear yet.

Concerning the pachyostosis of the mandible, there are different calculating methods. Young (1932) noted: “Index of thickness is meant the ratio between the height and the breadth of the jaw in the chosen place”, i.e., Mandible Pachyostosis Index = 100 × lingual depth / thickness, and it was followed and modified by Vislobokova (2013) as “the ratio of the jaw body depth (D) to its width (W) under M2 and M3 (100 D/W)”. van der Made and Tong (2008) also described the “robusticity” of the mandibles with the index 100 D/W, but it was measured under m3. On the contrary, Teilhard de Chardin (1936) proposed that “Mandibular Index = 100 × thickness under m3/internal depth under m3”, and it was followed by Ji (1988). None of the adult mandibles from SSMZ are preserved intact, they are either compressed or are broken. The specimen IVPP V 25966.15 is the most typical of its kind, although only the middle part was well preserved, the PI at m2 is 74.2 by Teilhard de Chardin’s method and 134.7 by Young and Vislobokova’s method, and both values are

prominently larger than that of a common deer.

3.2.3. Teeth

In SSMZ site, the majority of the teeth are still retained on the jaw bones, only very few of them are isolated from the bone. In individual numbers, juveniles are the dominants. All of the teeth, including deciduous and permanent teeth, got worn more or less, and most of them are moderately worn, which means that the animals died from unnatural death. There is no trace of a *Paleomeryx* fold on the lower molars.

3.2.3.1. Deciduous teeth

3.2.3.1.1. Deciduous upper dentition

Three partial maxillaries (IVPP V 25966.3, IVPP V 25966.9) with complete deciduous toothrows are available. From DP2 to DP4, both the size and the crown height increase; the length of the upper deciduous toothrow is 54.9–62.9 (Fig. 4; Table S4 in Supplementary data). There is no sign of cingulum on the deciduous upper teeth.

DP2: In occlusal view, the tooth looks quite elongated and the anterior portion is much narrower. Although the four main cusps are quite developed, the form is completely molarized. The paracone and the metacone are quite close to each other, and a prominent buccal rib corresponds with the paracone; parastyle is also quite developed; the protocone is somewhat isolated; the metaconule (or hypocone) is very robust and expanded, and is separated by a metaconule fold from the protoconule, the latter is also quite developed. In lingual view, the occlusal surface is prominently lower than those of DP3 and DP4.

DP3: In crown view, the tooth is fully molarized, but still has larger length than width, and the anterior lobe is remarkably narrower than the posterior one; with all the main cusps and styles well developed; three buccal ribs corresponding with the parastyle, paracone and mesostyle respectively are very outstanding; one specialty is the presence of a protocone fold posterior to the protocone in the lingual groove in some DP3, there exists a metaconule fold or spur in the posterior fossette.

DP4: As the largest tooth in the deciduous upper dentition, DP4 has larger width than length and with a more molariform shape; with four crescentic cusps and styles well developed; three buccal ribs corresponding with the parastyle, paracone and

mesostyle respectively are equally developed as in DP3; in DP4, the metaconule fold or spur in the posterior fossette is getting stronger. In one specimen (IVPP V 25966.7), DP4 has a developed entostyle (central lingual column by Lister, 1996).

3.2.3.1.2. Deciduous lower dentition

Seven partial mandibles (IVPP V 25966.4, IVPP V 25966.5, IVPP V 25966.20, IVPP V 25966.12, IVPP V 25966.21, IVPP V 25966.23, and IVPP V 25966.13) with complete or nearly complete deciduous toothrows are available. From dp2 to dp4, the size and the crown height as well as the complexity in structure increases remarkably; the length of the lower deciduous toothrow is 51.6–64.5 (Fig. 4; Table S5 in Supplementary data). No cingulid on the lower milk teeth was observed.

The dp2 is complicatedly constructed; the crown outline is in elongated triangular and the narrower portion points to the front (Fig. 1E); the cuspids are crest-like, the paraconid is shrinked but with a pronounced rib; the parastylid is not detected; the protoconid and metaconid are very weak, but the former represents the tallest part of the tooth; the hypoconid and entoconid are strong enough; the entoflexid and talonid basin are narrow and deep.

The dp3 is much more complicatedly constructed, and larger than dp2 (Fig. 3B3); the outline is in narrow trapezoid, with the lingual side concaved and the narrow portion toward anterior; all of the cuspids are equally developed; the valley between parastylid and paraconid is closed, and the entoflexid and the talonid basin are closed at deeper part; the buccal wall is flat but slightly convex, and the hypoflexid is quite shallow.

The dp4 is the most complicatedly constructed tooth which has three lobes (Fig. 4B3, C3), each lobe has a separate infundibulum, namely anterior, posterior and third fossettid respectively, and the three lobes are nearly equally developed but the posterior one is more expanded; the anterior lobe consists of anterobuccal conid and paraconid, the middle lobe consists of protoconid and metaconid, and the posterior lobe is composed of hypoconid and entoconid. On the buccal side, there are two basal pillars (anterior ectostylid and ectostylid). On the lingual side, the parastylid, mesostylid and metastylid are well developed, and the latter forms a pronounced rib; but the entostylid is not developed.

3.2.3.2. Permanent teeth

3.2.3.2.1. Permanent upper dentition

The premolars usually are single-lobed, and without any cingulum. The molars are double-lobed and with weak cingulum. Dimensions of the permanent teeth are shown in Table S6 in Supplementary data. The length of the premolar series is 58.6, and the length of the molar series is 73.6–75.2.

P2: only one specimen is available (IVPP V 25966.18) (Fig. 5B); the outline is in rhomboid and the length is larger than width; the four main cusps are well developed, the paracone and metacone form the buccal wall and represent the tallest part of the tooth, and the two cusps themselves are separated by a shallow valley, the paracone has a pronounced rib angling to the anterior; the protocone is the robustest cusp, which joints the parastyle and form the anterior wall together; the metaconule is teardrop shaped and nearly isolated, and connects with the protoconule at the deeper part; the parastyle rib is developed and is close to the paracone rib; the lingual groove is very deep.

P3: Two specimens are available for P3 (IVPP V 25966.18, IVPP V 25966.14) (Fig. 5B, C); the outline looks like that of P2, but its length is smaller than width, and the metacone and metaconule are remarkably shrank; the paracone represents the tallest part of the tooth, and the paracone rib is slightly far away from the parastyle rib but still located at the anterior portion; the metaconule has a long spur (or medial crista by Gustafson, 2015) extending posterobucally in the fossette; the lingual groove is shallow.

P4: Three specimens are available for P4 (IVPP V 25966.18, IVPP V 25966.14, IVPP V 25966.17) (Fig. 5A-C); it differs from P3 in much larger width and shortened length, the backward shifting of the paracone rib as well as the lack of lingual groove.

M1-2: Three specimens are available for M1-2 (IVPP V 25966.18, IVPP V 25966.14, IVPP V 25966.17) (Fig. 5A-C). The two teeth are very similar in form, but the former is prominently smaller. Both teeth with four crescentic main cusps well developed; the parastyle, paracone and mesostyle ribs are quite pronounced; the metaconule folds are weak. In buccal view, very weak horizontal basal ridges (Lister et al., 2005) can be observed between the mesostyle and paracone, and sometimes, the metastyle pocket as in modern Capreolinae (Gustafson, 2015) also can be detected. In lingual view, the entostyles are moderately developed; and the cingulum only occurs at each corner of the lingual side, the anterolingual cingulum is best developed; the

cingulum at the lingual groove is merged with the entostyle; the cingulum on M2 is much more developed than on M1. Some of the mesostyle rib may fork.

M3: Two specimens are available for M3 (IVPP V 25966.14, IVPP V 25966.17) (Fig. 5A, C). With similar size and constructions as M2, but the buccal ribs and entostyles are much more pronounced.

3.2.3.2.2. Permanent lower dentition

From p2 to m3, both the size and the complexity increase. The cingulid is not typically present on the buccal side, just some structure like the "goat fold" in *Capra* is present. From m1 to m3, the ectostylid on the buccal side reduces. The length of the premolar series is 53.6–54.1, and the length of the molar series is 83.8–85.8 (Table S7 in Supplementary data). The hypsodonty index of the m2 measured on specimen IVPP V 25966.11 is 0.9, which means *E. boulei* has mesodont teeth according to the criteria established by Fortelius et al. (2002).

p2: Two specimens are available for p2 (IVPP V 25966.16, IVPP V 25966.24) (Fig. 6A, C). The crown structure is very similar to that of dp2, only differences are its larger size, lower L/W ratio and more concaved trigonid basin. The anterior part is blade-like.

p3: Three examples are available for p3 (IVPP V 25966.15, IVPP V 25966.16, IVPP V 25966.24) (Fig. 6A-C). The crown structure is very similar to that of dp3, differs in its larger size and lower L/W ratio. The buccal wall is convex.

p4: Three specimens are available for p4 (IVPP V 25966.15, IVPP V 25966.16, IVPP V 25966.24) (Fig. 6A-C). The crown structure is completely different from that of dp4 in its form and lower L/W ratio; but similar to that of p3, except its slightly larger size, further lower L/W ratio, and the lingual enclosure of the talonid basin. The buccal wall is convex.

m1-2: Four specimens are available for m1-2 (IVPP V 25966.11, IVPP V 25966.15, IVPP V 25966.16, IVPP V 25966.24) (Fig. 6A-C). First and second molars are mutually similar in structure, both has two lobes, and the posterior lobe is slightly wider; the buccal cuspids include protoconid and hypoconid as well as the ectostylid between them; the lingual cuspids include metaconid and entoconid, the lingual cuspids are much robuster and much higher; but m1 is usually smaller than m2. On the lingual side, the parastylid and entostylid ribs are very pronounced.

m3: Three specimens are available for m3 (IVPP V 25966.15, IVPP V 25966.16,

IVPP V 25966.24) (Fig. 6A-C). The third lower molar resembles dp4 in morphology, but differs in its much larger size and relatively reduced third lobe; but the dental nomenclature of m3 is different from that of dp4. The buccal conids include protoconid, hypoconid and hypoconulid; the lingual conids include metaconid, entoconid and entoconulid; the third lobe (hypoconulid lobe) with a central fossettid; with pronounced parastylid and entostylid ribs.

3.2.4. Postcranial skeleton

3.2.4.1. Scapula

Only one specimen is available for scapula (IVPP V 25966.25) (Fig. 7A). It preserves the glenoid cavity, the neck and the basal part of the blade and the spine, but the acromion is broken off. In ventral view, the glenoid cavity is circular in outline and without a prominent glenoid notch, which is typical for cervids. In lateral and medial views, a pronounced coracoid process on the anterolateral margin of the glenoid fossa can be seen, which forms a notch with the glenoid cavity and is more developed than in other cervids; the neck portion is prominently constricted. In general look, it takes after the scapula of red deer. The smallest length and the lateromedial diameter of the neck are 40.0 and 24.3 respectively, the length and breadth of the glenoid cavity are 51.9 and 50.7 respectively.

3.2.4.2. Humerus

Only one specimen is available for humerus (IVPP V 25966.26) (Fig. 7D) with intact distal half. The outline of the shaft is in ellipse form, and the anteroposterior is along the long axis. In cranial view, there is a slight indentation above the articular surface which is called the radial (or coronoid) fossa; at the lateral one third of the trochlear surface, there exists a sharp sagittal ridge; no condyloid crest was detected above the epicondyle at the anterolateral aspect. In posterior view, the olecranon fossa is hollow and very deep; the medial epicondyle is much stronger than the lateral one, and the former is quite straight while the latter is inclined. In medial view, the ridge of the medial epicondyle forms a nearly right angle with the most distal margin of the humerus.

Dimensions: width of shaft at narrowest point = 40, anteroposterior diameter = 47.9; greatest breadth of the distal end = 75.3; greatest anteroposterior diameter of the

distal end = 73.5; greatest breadth of the trochlea = 63.0, tallest part of the trochlea is at the medial side and measures 53.1, the lowest part of trochlea measures 35.7.

3.2.4.3. Radius

Only one specimen is available for radius (IVPP V 25966.27), it is attached with the ulna, and both of them match well with the aforementioned humerus, thus they all belong to the same animal (Fig. 7B, C). The bones are seriously fractured. In general form, the radius is very slender, and the shaft is compressed anteroposteriorly and arched toward the front.

In proximal view, the medial glenoid cavity is remarkably larger than the lateral glenoid cavity, between them there exists a prominent articular groove, and a narrow notch occurs at the posterior end of the groove, which accommodates the lateral articular facet of the ulna, while another shallow notch exists at the anterior end of the groove; to the lateral side of the glenoid cavity, there is the lateral tuberosity which forms a quite large platform. In anterior view, the proximal end is expanded, but no radial tuberosity is detected; the shaft is straight; at the distal end there are three grooves: the extensor tendon groove, the maxillary groove (quite narrow) at the medial side and the groove for tendon of common digital extensor at the lateral side; the scaphoid articulation surface at the distal end represents the lowest part. In lateral and medial views, the interosseous space can be observed at the upper one third part of the bone. In distal view, three large articular surfaces can be recognized: the lateral cuneiform facet, the medial scaphoid and the lunate facet between them; all these three facets are irregular in shape and are running at different levels, and they are separated by sharp ridges; the scaphoid facet is much more extended downward; the lateral facet of radius joins the facet of the styloid process of distal ulna, both of them articulate with the cuneiform, but they are not fused together, which is different from that of bovids.

Dimensions: greatest length = 367.4, proximal width = 71.2, breadth of the humeral articular surface = 62.9, smallest breadth of diaphysis = 43.2, greatest breadth of the distal end = 64.8, greatest breadth of the distal articular surface = 59.9.

3.2.4.4. Ulna

Only one specimen is available for ulna (IVPP V 25966.27) (Fig. 7C). It’s seriously fractured, but with the two ends nearly completely preserved.

In anterior view, the anconaeus process part sharply thickened relative to the dorsal border of the olecranon process; the trochlear notch or semi-lunar notch lies directly distal to the anconeal process and is quite deep; the medial edge of the semi-lunar notch rolls medially; the medial articular facet is broken off; in the semi-lunar notch, the roof part is completely used as articular facet, but in the lower part, only the medial side has the articular facet which continues unbroken downward to the medial facet, but there exists a ridge between them.

In lateral view, the olecranon process has a quite straight dorsal border, a slightly concaved ventral border and a prominent notch at the tip. The angle of the anconaeus process between the semi-lunar notch and the dorsal border is around 90º; except the interosseous space part, other portion almost fused with the radius at the anteromedial side. In posterior view, the olecranon tuber part expanded more prominently than the other part of the olecranon process; the lateral portion of the coronoid process is more pronounced; the shaft is seriously flattened transversely and blade-like.

Dimensions: greatest length = 441.4, olecranon length = 87.3, smallest depth of olecranon = 58.0, the depth across processus anconaeus = 63.0, greatest breadth of the proximal articular surface > 35.0.

3.2.4.5. Metacarpals

Two complete Mc III+IV are present in the SSMZ collections (IVPP V 25966.28, IVPP V 25966.39) (Fig. 8A, B; Table S8 in Supplementary data). The two specimens are fairly well preserved, and they are quite slim and gracile, but quite long, representing the longest for fossil cervids ever reported in China.

In proximal view, two large articular facets form an asymmetric semicircular, the larger facet or magnum-trapezoid facet is relatively wide and has a curved edge, the smaller facet or unciform facet is triangular; between the two facets there exists a groove or depression which opens to the palmar aspect, but the nutrient foramen in the groove is tiny. The posterior medial tubercle is not noticeable. In anterior view, a narrow groove goes throughout almost the entire shaft, which ends at the nutrient foramen and represents the suture or fusion line between Mc III and IV; the cranial side is more rounded, the distal end has no vascular groove (or metacarpal gully) as in bovids, moreover the distal nutrient foramen is present although tiny. In posterior view, a small shallow groove can be observed between the two proximal facets; the shaft has a medial longitudinal depression on the upper three-fifth of the bone, and a

small nutrient foramen occurs at the upper end of the depression. A very tiny nutrient foramen exists near the distal end. The articular facet for the vestigial 5th metacarpal can be seen on one specimen (Fig. 8A4).

3.2.4.6. Tibia

Only two partial tibiae are available in the collection (IVPP V 25966.36, IVPP V 25966.31) (Fig. 7E). Both of them only preserved partial shaft and complete distal end.

In anterior view, the preserved shaft is massive and nearly straight, and the caudal aspect of the shaft is quite flat; near the distal articular surface, there is a prominent tubercle near the anterolateral border; the articular facets for lateral malleolus is located at a much higher position than the tips of the spine and medial malleolus, the latter two stand at nearly the same level or the mesial malleolus is the longer; the notch between the spine and the medial malleolus corresponds with the lateral ridge of the astragalus trochlea. In posterior view, some muscle scars can be seen on the front surface of the shaft. The posterior lower border is less downwardly extended. In lateral view, a notch can be seen, which separates the articular facet for lateral malleolus into two portions and accommodates the conical proximal projection of lateral malleolus. On the distal end, the articular grooves are parallel to the sagittal plane of the shaft, the medial groove is narrower but longer, the lateral groove is wider and shorter; between the two grooves, there exists a sagittal ridge, and on the anterior end of the ridge, there is a beak-like structure (the spine) which corresponds to the tibia trochlea of the astragalus. There are two small articular surfaces on the lateral edge for the attachment of the lateral malleolus (or distal fibula).

Dimensions: the greatest breadth of the distal end is 62.7–63.2, the greatest depth of the distal end is 48.1–49.3, the smallest breadth of diaphysis is 41.9.

3.2.4.7. Calcaneum

One calcaneum can be referred to the species (IVPP V 25966.46) (Fig. 7F). It was recovered before the systematic excavation, and is slightly broken at the calcaneal tuber part.

In anterior view, it is mediolaterally compressed in the shaft, but expanded at the tuber calcis (calcaneal head). At the upper part of the anterior process there is a trochlear facet (fibular condyles), which articulates with the distal surface of the

lateral malleolus. In posterior view, the calcaneal tuber has a shallow longitudinal groove at the tip, where the tendon of the gastrocnemius is attached to (the sulcus for the deep flexor tendon). The sustentaculum is moderately projected medially and with a nearly straight superior border. The cubonavicular facet is narrow and sloped. In medial view, the trochlear facet and the facet for the articulation of the astragalus are connected by a smooth articular surface. The astragalar facet meets the cubonavicular facet all the way. In lateral view, the calcaneal head has a notch at the anterior top, and the distal end is tapered; the proximal part of the lateral malleolus facet protruded pronouncedly and has a semi-circular outline. The anterior edge of the shaft is nearly straight, but the back edge is slightly curved. In distal view, the articular surface for astragalus (tibial tarsal) resembles a three-quarter circle, and the longer axis runs mediolaterally; the cubonavicular facet is a narrow belt which is also sloped anteroposteriorly; the anterior face of the lateral malleolus facet also can be seen.

Dimensions: the greatest length is 138.5, the greatest breadth is 37.9.

3.2.4.8. Astragalus

Three specimens of astragalus are available (IVPP V 25966.33, IVPP V 25966.34, IVPP V 25966.40, IVPP V 25966.41) (Fig. 7G), all of them are nearly completely preserved and the measurements are shown in Table S9 in Supplementary data.

In the anterior view, there are two proximal trochlear ridges (or condyles), which are parallel to one another and to the sagittal plane; the lateral ridge is slightly higher and narrower, and the lateral and medial borders of the trochlear condyles are straight. There is a deep saddle-like median groove between the two proximal trochlear ridges. At the distal part, the border of the distal articular surface is roundly convex, between the medial and lateral trochlear condyles, there is a broad shallow groove. In posterior view, the posterior articular surface for calcaneum is flat and slightly convex, but with a shallow longitudinal groove; the lateral edge is nearly straight; the medial bottom extends further downwards and meets the distal trochlear surface, but at the lateral bottom, there is a flange, which results in the separation of the distal trochlear surface from the calcaneum facet. The lateral face is trench-like and with anterior and posterior rims and flat floor; at the bottom, the facet of calcaneum is oval-shaped. There is no articular facet on the medial aspect.

3.2.4.9. Cubonavicular (fused central/fourth tarsal or naviculo-cuboid)

Only one perfectly preserved cubonavicular (IVPP V 25966.42) can be assigned to *E. boulei* (Fig. 7H).

In proximal view, the articular surface consists of a large trochlear facet with a pair of depressions and a distinct posterior beak-like projection, the depressions are astragalar facets; a narrow belt-like facet occupies all the lateral part, which articulates with the calcaneum. In distal view, the general outline of the distal surface is that of a rounded quadrilateral with two large anterior articular facets and two smaller facets. The anteromedial facet is articulated with fused 2nd and 3rd tarsals; the smallest facet articulates with 1st tarsal; the other two medial facets articulate with Mt III+IV. In posterior view, between beak-like projection and the calcaneal facet, there is a deep V-shaped notch. In anterior view, the facet articulated with fused 2nd and 3rd tarsals is higher in position than other distal facets. The calcaneal facet is sloping upward anteroposteriorly.

Dimensions: the greatest breadth is 55.9–57.4.

3.2.4.10. Metatarsals

Four nearly complete Mt III+IV (posterior canon-bone) are available (IVPP V 25966.45, IVPP V 25966.29, IVPP V 25966.44, IVPP V 25966.43) (Fig. 8C-E), two are long and another two are relatively short; the size differences can be tentatively attributed to sexual dimorphism. The measurements are shown in Table S8 in Supplementary data. In general, the proximal and distal articulations are less heavily built and narrow relative to the shaft.

At the proximal end, the medio-lateral dimension of the proximal end is smaller than the antero-posterior dimension. The proximal surface consists of four articular facets, and the anterior edge is roundish, while other margins are nearly straight; the two lateral facets are more elongated than the two medial ones; the two larger articular facets are oriented approximately parallel to the sagittal plane of the shaft, but not contact with each other; both of them have longer anteroposterior dimensions. The anteromedial facet articulates with the fused 2nd and 3rd tarsals; the anterolateral facet articulates with cubonavicular. There are two smaller facets located near the posterior margin; the posterolateral facet has larger medio-lateral dimension and articulates with cubonavicular; the smaller roundish facet articulates with the 1st tarsal. There is a large nutrient foramen positioned slightly off-center posteriorly.

From the nutrient foramen, three sulci are initiated. There is a nutrient foramen on the anterior and posterior aspect respectively, but the dorsal one is much smaller than the plantar one.

The shaft is slim, with deep dorsal groove and plantar longitudinal depression, the dorsal groove covers almost the entire shaft, but the plantar depression only occurs at the upper two-third of the shaft. In lateral view, the shaft is becoming compressed gradually downward, and the upper part has larger DAP than DT, but the lower part has larger DT than DAP.

At the distal end, there are two distal condyles, and the intercondylar margins of the condyles are parallel. On the anterior surface, the dorsal groove begins from the proximal nutrient foramen and runs throughout the whole shaft and stops at the distal nutrient foramen, but doesn't reach the intercondylar fossa as in bovids. In posterior view, a small distal nutrient foramen occurs very near to the distal epiphysis. In cross-sectional view of the midshaft, both of the anterior and posterior surfaces are concave, the former is narrow, but the latter is quite wide.

4. Comparisons

E. boulei is a large-sized deer endemic to continental Eurasia, therefore only the Eurasian cervids with similar body size, both extant and extinct, are compared in this section.

4.1. Comparison with the species of *Eucladoceros*

4.1.1. Comparison of the *E. boulei* specimens in China

Up to now, no more postcranial bones were reported for *E. boulei* in China, and most of the *E. boulei* fossil collections are represented by incomplete skulls, partial jaw bones and fragments of antlers (Young, 1935; Teilhard de Chardin and Trassaert, 1937; Chow and Chow, 1965; Chia and Wang, 1978; Tang, 1980; Tang et al., 1983; Zheng et al., 1985; Dong et al., 2017).

The SSMZ collection is significant in containing more specimens of dentitions (both deciduous and permanent), longer metapodials and the yearling antler; although the adult antlers are absent, the sizes and general characters of the dentitions and metapodials are very close to that of *E. boulei* described by Teilhard de Chardin and Piveteau (1930), except the more developed spurs on premolars in their type

specimens. However, the intraspecific variation for the fossils from the type locality is quite prominent; especially the antlers are much diversified (Teilhard de Chardin and Piveteau, 1930, pls. 8, 9), which was also noticed by Azzaroli and Mazza (1992a).

In addition to the type materials, the only available specimen for comparison is the maxillary with P3-M3 (V 5561) from Gonghe Basin in Qinghai Province, whose upper M1-3 length is 77.7 (Zheng et al., 1985), which is slightly larger than the Nihewan specimens.

With regard to the recently reported specimens from Chifeng in Nei Mongol (Dong et al., 2017), the identification is still open to question, because the measurements of the upper M3 do not coincide with that of a normal upper M3 of *E. boulei*; furthermore, the mandible and the lower molars are also quite different from those of the type specimens in morphology.

4.1.2. Comparison with *E. proboulei*

The identification of the recently named species *E. proboulei* Dong and Ye, 1996 is still open to question because of the following differences from the characters of the genus *Eucladoceros*: smaller size (same size as an extant sika deer estimated by antler size), shorter shaft (basal beam) and short beam, smaller angles between tines and beam, strong tines relative to beam, fewer prong numbers, lack of a bend of the beam at the brow tine, and pronounced grooves on the surface; furthermore, the species was only represented by a slightly deformed partial antler. Moreover, the *E. proboulei* was from the Lower Pliocene (ca. 5 Ma) (Dong and Ye, 1996), which is too early to be the direct ancestor of *E. boulei*. The present authors think *E. proboulei* resembles the European species *Croizetoceros ramosus* described by Heintz (1970) and Valli (2001) in antler morphology, but obviously larger, the latter was estimated to be 60 kg (Valli, 2001).

4.1.3. Comparison with other species of *Eucladoceros* from outside China

E. boulei was regarded as an "aberrant" species within its genus, and it differs from the European species in the following features: 1) high position of the outer tine (longer shaft); 2) inner tine generally strong; 3) crown tines inserted far back on the beam, occasionally tending to coalesce. The weight of the antlers is thus shifted backwards; this is compensated by a tendency of the beam to curve forwards (Azzaroli and Mazza, 1992a); furthermore, *E. boulei* has relatively short metapodials

and small deciduous teeth than *E. giulli* (Kahlke, 1997; van der Made and Dimitrijević, 2015), but longer metapodials and cheek toothrows than those of other European species (Heintz, 1970; de Vos et al., 1995; Croitor and Bonifay, 2001; Valli, 2001).

The general pattern of the antlers, together with the features of the skull and of the dentitions, shows an obvious relationship of the European species with the Chinese *E. boulei*, but at the same time they may have evolved quite differently. *E. boulei* represents a divergent clade. The lower portion of the antler with the outer tine high above the burr and the strong inner tine represent plesiomorphic features, while the richly branched crown tines are autapomorphic. The phyletic relationships between the several European species are far from clear but these species are fairly closely related among themselves. *E. falconeri* may be the common ancestor of all. *E. boulei* is separated from the European stock by distinct autapomorphies. A possible derivation of giant deer of the genus *Megaceroides* from some Asian species related to *E. boulei* is hypothesized (Azzaroli and Mazza, 1992b).

4.2. Comparison with selected megacerine taxa

4.2.1. *Sinomegaceros*

The Chinese giant deer (*Sinomegaceros*) are quite different from the European ones in having much developed brow tines and smaller body build (except *S. yabei*), and they are even smaller than *Eucladoceros*; furthermore, *Sinomegaceros* species have strongly palmated brow tine and other antler prongs, brow tine arises very close to the burr, skull is generally shortened but has larger zygomatic breadth, with brachydont teeth, strongly pachyostosed mandibles and massive limb-bones (Young, 1932).

The fossil records of *Sinomegaceros* in China mainly occur in the Middle Pleistocene, and the Late Pleistocene records are also quite often, but the species *S. konwanlinensis* from the Gongwangling human site is of an Early Pleistocene age (Chow and Chow, 1965; Zhu et al., 2015). Huang et al. (1989) proposed that the Chinese giant deer *Sinomegaceros* was derived from the local *Eucladoceros*; but others proposed that they were from the earlier *Sinomegaceros* species of Tajikistan (Vislobokova and Hu, 1990; Vislobokova, 2012).

4.2.2. *Arvernoceros*

Arvernoceros includes several diversified species with different forms and sizes, which makes it difficult or even confusing to compare. Currently, *Arvernoceros* was included in the genus *Rucervus* as a subgenus (Croitor, 2018b). The type species, *A. ardei*, is different from *E. boulei* in its longer beam and the three-tined palmation of the terminal tines (Heintz, 1970). Although *Eucladoceros* and *Arvernoceros* quite often coexisted in the Middle Villafranchian Khapry Faunistic Complex in the Sea of Azov Region (Baygusheva and Titov, 2013), there is no *Arvernoceros* ever reported in China except the species *Elaphurus bifurcatus* which was transferred to *Arvernoceros* by Croitor (2009).

4.2.3. *Praemegaceros*

The genus *Praemegaceros* also includes a complex of diversified species (Vislobokova, 2013), which makes it impossible to have specific comparisons between *Praemegaceros* species and *E. boulei*. No fossil of *Praemegaceros* was ever reported in China.

4.2.4. *Megaloceros*

The giant deer *Megaloceros giganteus* covered most part of continental Europe and Siberia during Late Pleistocene. The species of *Megaloceros* are characterized by large body mass, concaved frontal, circular cross-section of pedicle, ossified vomer, reduced ethmoidal orifices, pachyostosed mandible, absence of upper canine, molarized p4 (Croitor, 2018a); big antler which has very reduced brow tine but longer main beam as well as palmated terminal tines. In morphology of the postcranial bones, *E. boulei* is much closer to *M. giganteus* than to Alceini taxa (Breda, 2005), and it has been supposed that the ancestor of the group *Megaloceros giganteus* could have been closely related to *E. boulei* from China (Azzaroli, 1994). As a matter of fact, *E. boulei* has almost the same-sized metapodials as the early Middle Pleistocene *M. verticornis* (Dawkins, 1868) (Pfeiffer, 2002) and the Late Pleistocene *M. giganteus* from Dzhambul (Shpansky, 2014). Meanwhile, there is no report about the occurrence of this species in East Asia till now, and *Megaloceros* never overlapped with those of *E. boulei* in neither temporal nor spatial distributions.

4.3. Comparison with selected taxa of Alceini

4.3.1. *Libralces*/*Cervalces*/*Alces*

Alces alces and other Alceini taxa have obviously larger body size, longer muzzle part but very short nasal bones (except *Cervalces* according to Breda, 2008) than *E. boulei*; furthermore, the antler lacks a brow tine, pedicle and antler beam extend laterally in nearly a horizontal way; all the cheek teeth are brachyodont, and have lower length/width ratios; without upper canine; upper cheek teeth with robust stylar ribs and developed spurs in the fossae; the main cusps of upper molars are nearly separated. Breda (2008) also noticed that the premolar/molar length ratio is high, molarization of p3 and p4 is pronounced, and the molars of both species have low crowns with lingual and labial walls converging to the occlusal surface.

In China, the only extant and fossil species of Alceini is *Alces alces*, which only occurs in the northeastern extremity of China, and the fossil record is only limited to Late Pleistocene. Except some isolated specimens of Late Pleistocene in northeastern China, the Early and Middle Pleistocene fossil record of Alceini in China is completely unknown.

Although *Alces alces* is obviously larger than *E. boulei*, and is also different in antler shape and craniodental characters, Flerov (1952, p. 13) regarded *Eucladoceros* as a possible forerunner of *Alces*, but this viewpoint was not supported (Croitor, 2014); moreover, the present study also shows that *E. boulei* is a plesiometacarpal type, whereas *Alces* is a telemetacarpal type, which means *Eucladoceros* is distantly related to *Alces*.

4.4. Comparison with other large-sized Cervini taxa of Eurasia

4.4.1. The sambar deer (*Cervus* (*R.*) *unicolor*)

Sambar is the largest deer of the Oriental Region currently known, whose body is 225–320 kg for the male in India (Leslie, 2011), while the Chinese male only weighs 180 kg (Sheng, 1992). The Chinese sambar deer contains 4 subspecies, and almost all of them only distributed in southern China (Sheng, 1992).

C. (*R.*) *unicolor* can be distinguished from other species of Cervini by their robust, rugose antlers with a relatively long brow tine, very deep lacrimal pits, reduced auditory bullae, and dark eumelanic pelage (Groves and Grubb, 1987, p. 42, fig. 1); furthermore, Sambar is also characterized by its three-tined antlers among the

comparably sized Eurasian red deer and North American elk (Leslie, 2011) as well as the endemic white-lipped deer in China; the brow tine sits not far from the burr, and forms an acute angle with the beam that is forked at the tip.

The cheek teeth are large and with finely-wrinkled enamel, but slightly smaller than those of *E. boulei*; the upper premolars have pronounced lingual grooves; the upper molars bear robust and lingually forked entostyle; metaconid is fused with paraconid in p4; and the lower molars show developed precingulid and columned ectostylid (Zhang et al., 2018).

All of the craniodental and antler characters can be easily distinguished from those of *E. boulei*, although *Eucladoceros* have been proposed as possible ancestors of the living species *C.* (*R.*) *unicolor* (Leslie, 2011).

4.4.2. The white-lipped deer or Thorold's deer (*Cervus albirostris* = *Przewalskium albirostris*)

The white-lipped deer is endemic to the Qinghai-Tibetan Plateau in China and is a cold-adapted animal, whose average body weight of male is 205 kg. Skull has elongated and deep lachrymal pits (preorbital fossae); antler includes 4–7 prongs, and the beam is compressed or flattened, with no bez (second) tine, the brow tine arises at a considerably high position above the burr, the trez tine is nearly in the same plane with the tines above it, and the succeeding tine is longer than the others, the beam suddenly bents back at the origin of the trez-tine (Lydekker, 1898; Wu and Wang, 1999); each tine arises from the beam like an axil on the same plane (Ohtaishi, 1992), all of which are very similar to those of *E. boulei.*

Groves and Grubb (1987) thought *C. albirostris* shares the common ancestor with sambar. Recent studies show that *C. albirostris* has closer relationship with sika deer and red deer (Groves and Grubb, 2011). Because no fossil record was available, the evolutionary history of this species still remains unknown.

In tine numbers and inserting patterns as well as the compressed beam, *C. albirostris* is very similar to *E. boulei*, but the former's antler has shorter shaft and longer distance between brow tine and trez-tine as well as shorter metapodials.

4.4.3. Red deer (*Cervus elaphus*)

Red deer is a large animal whose stag's body weight is 200–250 kg; the Chinese red deer contains 8 subspecies distributed in northeastern and western China (Sheng,

1992).

The red deer is characterized by its large size and complex antler that is rounded throughout and normally has more than five points. When fully developed, the antler forms a more or less distinct cup at the crown, the brow tine rises close to the burr, and normally is longer than the bez, and the latter is very close to the brow tine. Upper canines present; upper molars are moderately tall, with a flattened additional column on the inner side (Lydekker, 1898).

The red deer is similar to *E. boulei* in tine numbers; but differs in lower positioned brow tine and bez-tine, rounded beam and crown tines; furthermore, all the craniodental dimensions of red deer are slightly smaller than those of *E. boulei*, especially the metapodials.

C. elaphus used to be the index fossil of Late Pleistocene in northern China, but it was recovered at the upper layers (1-3) of Peking Man site at Zhoukoudian, which is ca. 230–250 kyrs BP (Pei, 1939) and represents the earliest record of red deer in China, although its history can be traced back as early as ca. 1 Ma in Europe (van der Made and Dimitrijević, 2015); furthermore, the early representatives of red deer in China were also recovered in the Middle Pleistocene Jinniushan Site in Liaoning Province (Zheng and Han, 1993).

The fossil *C. elaphus* is different from *E. boulei* in the same aspects as the living forms, especially in its relatively hypsodont upper molars. Although it is proposed that all of the 12 *Eucladoceros* species have more or less the same size, and are comparable with *C. elaphus* (de Vos et al., 1995), the present study shows that *E. boulei*, whose body weight is 350 kg, is obviously larger than *C. elaphus* whose body weight is 200 kg (Kolb et al., 2015). The body weight of the European species of *Eucladoceros* is 250–300 kg (Croitor and Brugal, 2007).

4.4.4. Milu (*Elaphurus davidianus*) and other fossil and subfossil species

The species got extinct in the wild 100–200 years ago, but it survived in some nature reserves in China and some zoos around the world. The stag's body weight is 210–250 kg (Cao, 2005).

The specialized craniodental characters of *Elaphurus davidianus* can be summarized as follows: Antler dichotomously forked but without a brow tine, anterior prong extends upward and divided once or more, posterior prong projects backward at a large angle with the anterior prong simple or dichotomously branching; with

tubercles and longitudinal grooves on beam. The lower incisors and canines are hollowed, and from the canine to i1, the hollow is getting deeper; each hollow (or fossa) is divided into two unequal parts by a longitudinal crista, which is different from all other cervid taxa. The lower premolars have very reduced trigonid, and p4 has the anterior lobe molarized; lower molars without anterior cingulid, but have strong metastylids which results in a deep lingual groove, with pronounced lingual ribs; the lingual surface of the lower cheekteeth is not flat. Furthermore, some other important characters were also recognized by previous authors, such as the most special dental character is the internal enamel pillar on M2 and M3 (la cinquième et la sixième molaire), which is forked and with the anterior arm longer but the posterior arm shorter (Milne-Edwards, 1866); the lack of inflation of the auditory bullae (Groves and Grubb, 1987); incisiform teeth uniformly broad; hook-like sphenoid process; double channel in pedicle (Meijaard and Groves, 2004). It's worth emphasizing that the living species of *Elaphurus* has the most similar toothrow length with *E. boulei* (Table S10 in Supplementary data), which means that it's difficult to distinguish the teeth between the two taxa only by size.

Elaphurus menziesianus is a name given to the large deers unearthed from the Shang Dynasty site (ca. 3300 yrs BP) in Anyang, Henan Province. But they are actually very close to the extant species both in morphology and dimensions (Teilhard de Chardin and Young, 1936).

Although the fossil records of the genus *Elaphurus* can be traced back to the very early Pleistocene, the systematic position and origination of *Elaphurus* is still far from clear. Lydekker (1898) noted that the genus *Elaphurus* had nothing to do with any of the Old World Deer (Heckeberg, 2017). There is no stag whose systematic position has troubled zoologists as much as *Elaphurus* (Wemmer, 1983). Pitra et al. (2004) suggested that *Elaphurus davidianus* had a hybrid origin: the hybridization supposedly occurred between *Cervus canadensis* and *Cervus eldii* (= *Panolia eldii*), an endemic species in Southeast Asia.

The species *El. bifurcatus* Teilhard de Chardin and Piveteau (1930) once coexisted with *E. boulei* in Nihewan fauna, and both of them are large-sized deer; therefore, it is reasonable and necessary to compare the two taxa. But it is unfortunate that no other fossils are available except the antler specimens for *El. bifurcates* (Young, 1935; Chow and Chow, 1965; Chi, 1975; Chia and Wang, 1978; Wang, 1988), even though the most recent publication on *Elaphurus* classified the fossil

Elaphurus of east Asia into 4 species and 8 subspecies (Dong et al., in press), the knowledge about its skull and dentitions as well as postcranials is still completely unknown in China. Nonetheless, based only on the antlers, *El. bifurcatus* can be easily distinguished from *E. boulei*.

The Early Pleistocene Japanese species *Elaphurus shikamai* is also only represented by antlers, and it is closely related to *El. bifurcates* from Nihewan (Otsuka, 1972). The probable ancestor of *El. bifurcatus* is *Elaphurus eleonorae* from the Early Pleistocene of Kuruksay, Tadjikistan in Central Asia (Dong et al., in press).

In summary, *Elaphurus* has close toothrow length with *E. boulei*, but the former has much shorter metapodials and quite special antler and tooth forms. The comparisons between *E. boulei* and the Early Pleistocene *Elaphurus* species are still superficial, due to insufficient fossil materials and the uncertain phylogeny of the Early Pleistocene *Elaphurus* taxa.

4.5. Comparison with the Villafranchian three-tined deer

In northern China, the Villafranchian three-tined deers were quite diversified, and they were once referred to the following genera: *Axis*, *Cervus* (*Rusa*) and *Cervus* (*Deperetia*) (the subgeneric name *Deperetia* was replaced by *Nipponicervus* and was raised to generic level later on). Although Shikama (1941) has given an illustrated comparison among such three-tined taxa as *Axis*, *C.* (*Rusa*) and *C.* (*Deperetia*) in antler structures, the classification and phylogenetic relationships among them are far from clear. It's worth mentioning that there is no post-Pliocene fossil record of *Cervavitus* in northern China.

Axis shansius, a common species of Early Pleistocene in northern China, is obviously different from its extant co-generic species in relatively large body size and high positioned brow tine. Up to now, most of the knowledge about this species is limited to antlers, partial cranial specimens and dentitions, which are distinctly different from *E. boulei*.

The *Rusa* cf. *elegans* described by Teilhard de Chardin and Trassaert (1937) was renamed as *C.* (*Deperetia*) *trassaerti* by Shikama (1941), which is averagely larger than an extant sika deer, but similar to *A. shansius* and *Nipponicervus* species.

C. (*R.*) *elegans*, currently revised as *Nipponicervus elegans* by Qiu et al. (2004), frequently coexisted with *E. boulei* in northern China, but it's a medium to large-sized deer (ca. 150 kg) based on its toothrow length and metapodial length (Table S10 in

Supplementary data), and it can be easily distinguished by its simple three-tined antlers.

Nipponicervus longdanensis is a large-sized deer also with three-tined antlers, and it can be told from other large-sized rusine taxa by its higher positioned brow tine and generally slimmer antler, i.e., with longer shaft. It should have a similar body mass as the extant red deer according to it toothrow length.

The present authors think that *A. shansius*, *D. trassaerti* and *N. longdanensis* share almost the same shape of antler and similar body size, thus their taxonomic designation should be reconsidered.

As regard to the true rusines, taxa under the subgenus *C.* (*Rusa*) usually only occur in southern China. The Early Pleistocene species *C.* (*R.*) *yunnanensis* Lin et al., 1978 is originally represented by one incomplete antler as type specimen; but the large deer specimens from the *Gigantopithecus* Cave in Guangxi were also referred to this species, which is larger than *C.* (*R.*) *elegans* but smaller than *C.* (*R.*) *unicolor*, the latter frequently appeared in the Middle–Late Pleistocene sites in southern China (Han, 1987).

For *Rusa pachygnathus* Zdansky, 1925, it seems a good solution to transfer it to the genus *Sinomegaceros* because of its pachyostosed mandibles and similar postcranial size. But the the true identification of the mandible specimen from Hu-lu-tao in Huailai County (Zdansky, 1927) (not far away from Nihewan Basin) should be reconsidered, because its mandible is less pachyostosed and the geologic age is earlier. Further study may turn out that it represents an early form of *Sinomegaceros*, or it has some relationship with *E. boulei*.

5. Discussions

5.1. Body size versus toothrow and metapodial lengths

The metapodials of *E. boulei* are larger than those of the extant species of *Cervus*, and also larger than those of most co-generic species and even some species of Megacerines; moreover, the metapodials of *E. boulei* are relatively gracile (van der Made and Tong, 2008; van der Made, 2015, in press).

Although the living species of *Elaphurus* has the most similar toothrow length with *E. boulei*, the metapodials of the former are obviously shorter than those of the latter; on the other hand, *C. elaphus* has larger toothrow length but shorter metapodial

and smaller body size than *E. boulei* (Table S10 in Supplementary data), which means toothrow length and metapodial length are not always changing in same proportion among the animals (Fig. 9), although both of them are related to body mass (or weight) to a great extent. It was proposed that in limb-segment proportion, *C elaphus* and *E. davidianus* are very similar to that of *Eucladoceros* (Heintz, 1970, p. 208).

E. boulei is the largest fossil deer ever found in China, but it was only estimated by its larger toothrow and metapodial lengths, and its exact body mass is still unclear. We know that the methods for body mass estimation are various, both tooth and postcranial bones were used. In our study, the tooth seems not so reliable for body mass estimation, therefore, we chose the metapodials. Although metacarpals tend to be long in Cervinae and shorter in Alceinae-Rangiferinae (Frick, 1937), metapodials are still quite often chosen for body mass estimation (Purdue, 1987; Vukičević et al., 2012; Morris and Mead, 2016). In our study, it seems that metapodials' dimensions closely related to body mass (Fig. 9; Table S10 in Supplementary data).

The body mass of the related European taxa is 385 kg for *E. giulii* (Palmqvist et al., 2003), and 250 kg for *E. ctenoides* (Croitor and Brugal, 2007). Because the major dimensions of *E. boulei* are between those of the two species (Heintz, 1970; Kahlke, 1997; Valli, 2001).the body mass of *E. boulei* should be between 250 and 385 kg. In fact, our calculated body mass based on metacarpal length is ca. 350 kg.

Although Azzaroli and Mazza (1992a) noticed a decrease of the premolar row length/molar row length ratios, from Saint Vallier, via La Puebla de Valverde and Senèze, 79.22, 73.8 and 72.94 in the upper dentitions, and from 68.11 to 66.14 to 65.15 in the lower dentitions; our study shows the premolar/molar ratio is not a stable character for classification (Table S10 in Supplementary data).

The largest pre-Villafranchian cervid taxon in northern China is the three-tined *Axis shansius* whose body weight is larger than a sika deer (Dong, 1993), and estimated to be ca. 150 kg in this study. It was regarded as the ancestor of all the species of the genus *Axis* (Di Stefano and Petronio, 2002). The sudden appearance of such large-sized deer as *Eucladoceros* and *Elaphurus* may have represented a big migration event at the beginning of the Quaternary Period, in which other taxa were also involved, such as *Mammuthus*, *Equus*, and *Bison* etc.; and all of the aforementioned taxa not only appeared in Nihewan Basin, but also in Yushe Basin (Tedford et al., 1991). In Europe, the large-sized ruminants doubled their body weight during the early Pleistocene in order to adapt to the arid and more open environment

(Croitor and Brugal, 2007). Therefore, the appearance of very large deer can be employed to mark the beginning of the Quaternary Period in Eurasia. Furthermore, the quaternary cervid taxa are not only typical of their larger body size, but also for their multi-tined and/or palmated antlers (Fig. 10).

5.2. Mandibular pachyostosis

The pachyostosed mandible in some cervids has been widely noticed (Lister, 1994; Kahlke, 1997; van der Made and Tong, 2008; Vislobokova, 2013; Croitor, 2016), such as *Megaloceros*, *Praemegaceros*, and *Megaceroides*. The *Megaloceros* species are characterized by the well-known pachyostosis of the skull and, in particular, of the horizontal mandibular ramus. The latter feature is also documented in some species of *Praemegaceros* but at a lower degree (Abbazzi, 2004). This feature is prominently developed in *Sinomegaceros pachyosteus* (Young, 1932; Kahlke, 1958).

Pachyostosed mandible is one of the diagnostic character for Megacerini deer (Vislobokova, 2009, 2013), and it also less prominently occurs in *Eucladoceros*, which is the reason why the genus once was thought to be the forerunner of the giant deer *Megaceroides* (Azzaroli and Mazza, 1992b). Vislobokova (2013) emphasized the differences between *Eucladoceros* and the Megacerini deer in cranial characters. The cause of the pachyostosis of mandible is still under debate. Pachyostosis of mandible has also been observed in some large deer, and some fossil camel (Martini and Geraads, 2018).

Although the deer with pachyostosed jaws survived into the Holocene Epoch, there is no such kind of example in the living forms; therefore, the real cause of the pachyostosis is still open to question.

5.3. On taxonomy and phylogeny

The Late Miocene Cervinae in China was represented by three-tined deer (incorrectly identified with *Cervocerus novorossiae* before but currently assigned to *Cervavitus novorossiae* by Dong, 2011, Wang and Zhang, 2014) which gave rise to most of the Pleistocene and living Cervinae taxa (Azzaroli, 1953). The history of the Cervinae during the Pliocene is obscure (Azzaroli, 1953). The present authors think that the early Villafranchian is a bottleneck period for cervid evolution in northern China, which is characterized by the following features: decrease of cervid diversity,

disappearance of both the archaic groups and the population of the medium to large-sized three-tined deer (Fig. 10). The taxonomy of the Villafranchian large-sized deer in China is fairly simple compared to that of European forms. Only two genera, *Eucladoceros* and *Elaphurus*, have been identified in China. The latter can be easily distinguished from the former by its obvious smaller body size.

E. boulei has been verified as a plesiometacarpal deer by the occurrence of the facet of lateral metacarpal on the anterior cannon bone (Fig. 8A4), therefore, its taxonomic and phylogenetic positions should be among the Eurasian taxa. However, the exact phylogenetic position of *Eucladoceros* species within Cervini has often been controversial. *Eucladoceros* is not included into the Megacerines (Vislobokova, 2013), although a close relationship with this group has been proposed by Azzaroli and Mazza (1992b). Symplesiomorphic characters and a common evolutionary trend towards large size and heavy antlers could account for this. A close affinity of *E. ctenoides* from Senèze (in France) with *C. elaphus* is possible (Mennecart et al., 2017).

Flerov (1952, p. 13) regarded *Eucladoceros* as a forerunner of large-sized Quaternary cervid genera *Megaloceros*, *Cervalces* and *Alces*. The antler morphology of *E. ctenoides* resembles to a certain extent the antlers of modern *Przewalskium albirostris*. Croitor (2014) cautioned that the similarity in antler shape between *Eucladoceros* and *Przewalskium* may be superficial and in this case the assignment of *Eucladoceros* to the lineage *Przewalskium-Rusa-Cervus* is inappropriate. However, the analysis of body labyrinth morphology revealed a close affinity between *E. ctenoides* and *C. elaphus* (Mennecart et al. 2017), which may suggest that the observed similarity of the comb-like antler shape of *Eucladoceros* and modern *Przewalskium* is not superficial and supports the close relationship between these genera (Croitor, 2018a, p. 78).

The megacerine phylogeny, when it is based only on European species, is very incomplete. It was supposed that the group of *M. giganteus* was of uncertain origin and the group of *M. verticornis* (here *Praemegaceros verticornis* group) was derived from *Eucladoceros* (Azzaroli, 1953; Azzaroli and Mazza, 1992b; Abbazzi, 2004; Vislobokova, 2009).

Therefore, *Eucladoceros* is close either to the *C. albirostris-C. elaphus* group or to the fossil form of *Praemegaceros*.

The origin of *Eucladoceros* in northern China has been speculated either from

Siberia (Vislobokova, 2008a) or is endemic and derived from the Early Pliocene local taxon *Eucladoceros proboulei* from Yushe Basin (Dong and Ye, 1996). *Eucladoceros* is still regarded as the most important representative of Early Pleistocene in North China.

5.4. On the chronology of *Eucladoceros* species

Although it is supposed that *Cervavitus* gave rise not only to the tribe Megacerini, but also to a number of extinct (*Eucladoceros*) and extant genera (*Axis*, *Dama*, *Cervus*, *Elaphurus*) of the tribe Cervini (Flerov, 1952; Petronio et al., 2007; Vislobokova, 2012), the origin of *Eucladoceros* is still not quite clear. The earliest records of *Eucladoceros* are known from the Middle Pliocene or Early Villafranchian (MN16: 3.6–2.6 Ma) of Ukraine, Georgia, and Azerbaijan (Vislobokova, 2008a, 2008b); but in most part of Eurasia, its first appearance usually was employed to mark the beginning of the Quaternary Period or MN17 in Europe and Asia, which is 2.6 Ma (Vislobokova, 1990).

The arrival time of *Eucladoceros* in Western Europe from northern Eurasia corresponds with MN17, about 2.6–2.2 Ma (Agusti et al., 2001; Vislobokova, 2008a; Croitor, 2009). The genus is the only large mammal taxon chosen to mark the beginning of MN17 in western Europe.

In the Iberian Peninsula, *Eucladoceros* usually made its first appearance with *Equus* and *Mammuthus*, which is called the Elephant-*Equus* event, just slightly before the boundary of Early and Middle Villafranchian, i.e., earlier than 2.6 Ma (Madurell-Malapeira et al., 2014).

The Montopoli fauna and the related faunal unit occurring at the Gauss-Matuyama transition demonstrated the dispersal of the primitive mammoth (*M. meridionalis gromovi*), the true horse (*Equus* cf. *livenzovensis*), the ‘giant deer’ (*Eucladoceros*), and a *Gazella* (*G. borbonica*) into Italy (Masini and Sala, 2007).

Eucladoceros is an abruptly emerged species of large-sized deer at the beginning of Quaternary in China, its fossils can be easily recognized and are very helpful in determining the Early Pleistocene strata. Furthermore, it was also involved in the large mammal migration event, and can be employed as representative taxon for inter-regional correlation and paleobiome reconstruction. The immigration, nominally defined as “the Elephant-*Equus* dispersal event”, can be placed between 2.6–2.5 Ma and has an Asian origin. The event is characterized by the incorporation in the record

of *Eucladoceros*, monodactyl equids (*Equus*), another medium-sized cervid (*Metacervocerus*), and the first elephants of the genus *Mammuthus*. This dispersal would signify the replacement in the continental ecosystems of Europe of the mastodon genus *Anancus* by the first elephants (despite the fact that some subsequent deposits show the coexistence of both proboscideans, for example at Saint Vallier) and of the tridactyl equids (*Hipparion*) by monodactyls (Arribas et al., 2009).

The faunal sequence in Sésklo shows *Hipparion* did not co-occur with the stenonid horse, at least not in this region (Athanassiou, 2018), while other study shows "*Hipparion* and *Equus* horses could have coexisted in Europe up to the complete extinction of *Hipparion* in early Matuyama times" (Pueyo et al., 2016).

The "end-Villafranchian event" is marked by the extinction of the majority of Villafranchian ruminant species, like *E. ctenoides*, *Metacervocerus rhenanus*, *Praemegaceros obscurus*, small-sized Villafranchian *Cervus* and *Dama*, *Eobison tamanensis*. But *Leptobos* and *E. dicranios* became extinct somewhat earlier (Brugal and Croitor, 2007; Heckeberg, 2017).

The appearance of *Eucladoceros* together with *Equus*, *Youngia*, *Borsodia*, *Microtus*, *Trogontherium*, *Marmota* and *Bison* in the Nihewanian North China Mammal age marks the beginning of the Quaternary Period in East Asia, whose basal age is about 2.6 Ma (Woodburne et al., 2013).

It was generally agreed that the Nihewan beds represent the Early Pleistocene deposits in the Basin (Min et al., 2015), but the faunal composition analysis shows that Nihewan Fauna can be compared with Olivola Fauna in Italy (Qiu, 2000, 2006) and the recent paleomagnetic dating gives its age ca. 1.7–2.2 Ma (Liu et al., 2012), which shows that the *Eucladoceros* fossils from Nihewan Basin do not represent the earliest record of this taxon. Its occurrence in Yushe Basin is more likely the earliest *Eucladoceros* in China.

5.5. On the paleoenvironmental significance of *Eucladoceros* species

The paleoenvironmental significance of *Eucladoceros* is still open to question. The cranial morphology and tooth wear of *Eucladoceros* species are more similar to those of browsers than mixed feeders (Valli and Palombo, 2005). On the other hand, Berlioz et al. (2018) proposed that *E. ctenoides* is as plastic as the extant red deer *Cervus elaphus* in feeding habits: it was believed to be a browser at Chilhac of wooded habitats; while its diet at Saint-Vallier and Senèze may have contained high

percentage of herbaceous monocotyledons of open habitats.

Meanwhile, Vislobokova (2012) proposed that the Early Pleistocene *Eucladoceros* inhabited the southern part of northern Eurasia with *Alces* as well as the megacerine genera *Sinomegaceros*, *Praemegaceros* and *Megaloceros*, all of them are larger than the extant red deer. The appearance of those giant deer in the Plio-Pleistocene corresponded with the progressive cooling and seasonality as well as the relatively open habitats.

E. boulei in Nihewan basin usually co-existed with such species as *Ochotonoides* sp., *Proboscidipparion* sp., *Equus sanmeniensis*, *Mammuthus trogontherii*, *Coelodonta nihowanensis*, *Elasmotherium peii*, *Gazella sinensis*, *Bison palaeosinensis*, and diversified canids, which may indicate a steppe-dominated or quite open habitat.

6. Conclusion

The Early Pleistocene cervids from Nihewan Basin were quite diversified, among which *E. boulei* was the most important species. Based on toothrow length and the dental characters as well as the postcranial bone, the recently recovered large-sized cervid fossils from SSMZ in Nihewan Basin can be referred to the species *E. boulei*. Its body weight can be estimated to be ca. 350 kg and the species represents the largest Pleistocene cervid ever recovered in China. Besides the large size and peculiar comb-like antlers, *E. boulei* is also characterized by the pronounced anterior cingulids and entostylid ribs on lower molars as well as the moderately pachyostosed mandibles. The present study shows that the body weight of large cervids can be estimated by the toothrow length and metacarpal length. *E. boulei* is a typical element of the Early Pleistocene fauna in North China. The present study shows the early Villafranchian is a bottleneck period for cervid evolution in northern China, which is characterized by the following features: decrease of cervid diversity, disappearance of archaic groups and the rise of the medium to large-sized three-tined cervines. The very large-sized and/or multi-tined cervids, however, appeared suddenly at the Pliocene–Pleistocene transition, which may indicate a big mammal migration event.

Acknowledgements

The authors wish to express their thanks to the following people and organizations for their help: Fei Han, Bo-Yang Sun, Xi Chen, Xiao-Min Wang, Dan Lü, Ji-Jia Sun,

Zhi-Jun Xu, Zhen-Wei Qiu, Qiu-Yuan Wang, Bao-Hua Sun, Nan Hu, Xian-Ting Liu and Chao Yin, for participating the excavations; Fei Xie of HPICR, Wen-Jian Zhao of NNNRM and Wen-Yu Hou of NM for help during excavations; Yu-Guang Zhang of BMNH, Min Zheng of TNHM, C. Argot of MNHN, for providing access to collections; Zhan-Xiang Qiu, I.A. Vislobokova, J. van der Made, R. Croitor, V. Titov, Wei Dong, Qi Wei, and N.S. Heckeberg, for sharing bibliographies and/or for fruitful discussions; Ye-Mao Hou for CT scanning; J. van der Made and R. Croitor for constructive suggestions; Prof. Rongyu Li for polishing the English text. This work was supported by the following grants: The Strategic Priority Research Program of Chinese Academy of Sciences (Grant No. XDB26000000); the National Natural Science Foundation of China (Grant No. 41572003); the Special Basic Research Project (Grant No. 2014FY110300) of MST of China.

References

Abbazzi, L., 2004. Remarks on the validity of the generic name *Praemegaceros* Portis 1920, and an overview on *Praemegaceros* species in Italy. Rendiconti Lincei 15 (2), 115–132.

Agustí, J., Cabrera, L., Garcés, M., Krijgsman, W., Oms, O., Parés, J.M., 2001. A calibrated mammal scale for the Neogene of Western Europe: State of the art. Earth-Science Reviews 52, 247–260.

Arribas, A., Garrido, G., Viseras, C., Soria, J.M., Pla, S., 2009. A mammalian lost world in Southwest Europe during the Late Pliocene. PloS One 4 (9), e7127, doi: 10.1371/journal.pone.0007127.

Athanassiou, A., 2018. A Villafranchian *Hipparion*-bearing mammal fauna from Sésklo (E. Thessaly, Greece): Implications for the question of *Hipparion–Equus* sympatry in Europe. Quaternary 1 (2), 12, doi: 10.3390/quat1020012.

Azzaroli, A., 1953. The deer of the Weybourn Crag and forest bed of Norfolk. Bulletin of the British Museum (Natural History), Geology 2 (1), 1–96.

Azzaroli, A., 1994. Forest bed elks and giant deer revisited. Zoological Journal of the Linnaen Society 112, 119–133.

Azzaroli, A., Mazza, P., 1992a. The cervid genus *Eucladoceros* in the early Pleistocene of Tuscany. Paleontografia Italica 79, 43–100.

Azzaroli, A., Mazza, P., 1992b. On the possible origin of the giant deer genus *Megaceroides*. Rendiconti Lincei 9 (3), 23–32.

Bärmann, E.V., Rössner, G.E., 2011. Dental nomenclature in Ruminantia: Towards a standard terminological framework. Mammalian Biology – Zeitschrift für Säugetierkunde 76 (6), 762–768.

Baygusheva, V.S., Titov, V.V., 2013. Large deer from the Villafranchian of eastern Europe (Sea of Azov Region): evolution and paleoecology. Quaternary International 284, 110–122.

Berlioz, É., Kostopoulos, D.S., Blondel, C., Merceron, G., 2018. Feeding ecology of *Eucladoceros ctenoides* as a proxy to track regional environmental variations in Europe during the early Pleistocene. Comptes Rendus Palevol 17 (4–5), 320–332.

Breda, M., 2005. The morphological distinction between the postcranial skeleton of *Cervalces*/*Alces* and *Megaloceros giganteus* and comparison between the two Alceini genera from the Upper Pliocene–Holocene of Western Europe. Geobios

38, 151–170.

Breda, M., 2008. Palaeoecology and palaeoethology of the Plio-Pleistocene genus *Cervalces* (Cervidae, Mammalia) in Eurasia. Journal of Vertebrate Paleontology 28 (3), 886–899.

Brown, W.A.B., 1991. Age assessment of red deer (*Cervus elaphus*): from a scoring scheme based on radiographs of developing permanent molariform teeth. Journal of Zoology 225 (1), 85–97.

Brown, C.L., Gustafson, C.E., 1979. A Key to Postcranial Skeletal Remains of Cattle/Bison, Elk, and Horse. Reports of Investigations (Washington State University, Laboratory of Anthropology), No. 57, 199 pp.

Brugal, J.-P., Croitor, R., 2007. Evolution, ecology and biochronology of herbivore associations in Europe during the last 3 million years. Quaternaire 18 (2), 129–152.

Bubenik, A.B., 1990. Epigenetical, morphological, physiological, and behavioral aspects of evolution of horns, pronghorns, and antlers. In: Bubenik, G.A., Bubenik, A.B. (Eds.), Horns, Pronghorns, and Antlers. Springer-Verlag, New York, pp. 3–113.

Cao, K.Q., 2005. Research on the Milu. Shanghai Science and Technical Publishers, Shanghai, 246 pp. (in Chinese, with English summary).

Chi, H.X., 1975. The lower Pleistocene mammalian fossils of Lantian District, Shensi. Vertebrata PalAsiatica 13 (3), 169–177 (in Chinese, with English abstract).

Chia, L.P., Wang, C., 1978. Hsihoutu — A Culture Site of Early Pleistocene in Shansi Province. Cultural Relics Publishing House, Beijing, 85 pp. (in Chinese, with English summary).

Child, K.N., Aitken, D.A., Rea, R.V., 2010. Morphometry of moose antlers in central British Columbia. Alces 46, 123–134.

Chow, M.C., Chow, B.S., 1965. Notes on Villafranchian mammals of Linyi, Shansi. Vertebrata PalAsiatica 9 (2), 223–234 (in Chinese, with English summary).

Croitor, R., 2009. Phylogeny and speciation in the Quaternary cervid genera *Eucladoceros* and *Praemegaceros* (Cervidae, Mammalia). In: Bucar, I.I., Sasara, E., Pop, D. (Eds.), Seventh Romanian Symposium on Palaeontology Cluj-Napoca, 22-24 October 2009. Presa Universitară Clujeană, Cluj-Napoca, pp. 29–30.

Croitor, R., 2014. Deer from Late Miocene to Pleistocene of Western Palearctic:

matching fossil record and molecular phylogeny data. Zitteliana B 32,115–153.

Croitor, R., 2016. Systematical position and paleoecology of the endemic deer *Megaceroides algericus* Lydekker, 1890 (Cervidae, Mammalia) from the Late Pleistocene–early Holocene of North Africa. Geobios 49 (4), 265–283.

Croitor, R., 2017. Description of a new deer species (Cervidae, Mammalia) from the Early Pliocene of eastern Europe, with a review of early dispersals and palaeobiogeography of the subfamily Cervinae. Neues Jahrbuch für Geologie und Paläontologie, Abhandlungen 283 (1), 85–108.

Croitor, R., 2018a. Plio-Pleistocene Deer of Western Palearctic: Taxonomy, Systematic, Phylogeny. Institute of Zoology of the Academy of Sciences of Moldova, Chişinău, 140 pp.

Croitor, R., 2018b. A description of two new species of the genus *Rucervus* (Cervidae, Mammalia) from the Early Pleistocene of Southeast Europe, with comments on Hominin and South Asian ruminants dispersals. Quaternary 1 (2), 17, doi: 10.3390/quat1020017.

Croitor, R., Bonifay, Y.M.-F., 2001. Étude préliminaire des cerfs du gisement Pleistocène inférieur de Ceyssaguet (Haut-Loire). Paleo 13, 129–144.

Croitor, R., Brugal, J.-P., 2007. New insights concerning Early Pleistocene cervids and bovids in Europe: dispersal and correlation. Courier Forschungsinstitut Senckenberg 259, 47–59.

Damuth, J., Macfadden, B.J., 1990. Body Size in Mammalian Paleobiology: Estimation and Biological Implications. Cambridge University Press, Cambridge, 397 pp.

Dawkins, W.B., 1868. On a new species of fossil deer from Clacton. Quarterly Journal of the Geological Society of London 24, 511–516.

Degmečić, D., Florijančić, T., Ozimec, S., Bošković, I., Budor, I., 2013. Age determination of red deer (*Cervus elaphus* L.) stags in the Baranja region (Eastern Croatia) using the parameters of pedicles. In: Marić, S., Lončarić, Z. (Eds.), Fisheries, Game Management and Beekeeping: 48th Croatian & 8th International Symposium on Agriculture, Osijeku. Faculty of Agriculture of University of Josip Juraj Strossmayer, Osijek, pp. 667–671.

de Vos, J., Mol, D., Reumer, J.W.F., 1995. Early Pleistocene Cervidae (Mammalia, Artiodactyla) from the Oosterschelde (the Netherlands), with a revision of the cervid genus *Eucladoceros* Falconer, 1868. Deinsea 2, 95–121.

Di Stefano, G., Petronio, C., 2002. Systematics and evolution of the Eurasian Plio-Pleistocene tribe Cervini (Artiodactyla, Mammalia). Geologica Romana 36, 311–334.

Dong, W., 1993. The fossil records of deer in China. In: Ohtaishi, N., Sheng, H.L. (Eds.), Deer of China. Elsevier Science Publishers B.V., Amsterdam, pp. 95–102.

Dong, W., 2004. The dental morphological characters and evolution of Cervidae. Acta Anthropologica Sinica 23 (Suppl.), 286–295 (in Chinese, with English abstract).

Dong, W., 2011. Reconsideration of the systematics of the Early Pleistocene *Cervavitus* (Cervidae, Artiodactyla, Mammalia). Estudios Geológicos 67 (2), 603–611.

Dong, W., Ye, J., 1996. Two new cervid species from the Late Neogene of Yushe Basin, Shanxi Province, China. Vertebrata PalAsiatica 34 (2), 135–144 (in Chinese, with English summary).

Dong, W., Zhang, L.M., Liu, W.H., 2017. New material of the Early Pleistocene mammalian fauna from Chutoulang, Chifeng, eastern Nei Mongol, China and binary faunal similarity analyses. Vertebrata PalAsiatica 55 (3), 257–275.

Dong, W., Wei, Q., Bai, W.P., Zhang, L.M., Liu, W.H., Chen, Z.Y., Bai, Y.B., Wu, Y.C., in press. New material of the Early Pleistocene *Elaphurus* (Artiodactyla, Mammalia) from North China and discussion on taxonomy of *Elaphurus*. Quaternary International, doi: 10.1016/j.quaint.2018.05.015.

Falconer, H., 1868. Notes on fossil species of *Cervus*, including a description of a remarkable fossil antler of a large species of extinct *Cervus*, *C*. (*Eucladoceros*) *sedgwickii*, in the collection of the Rev John Gunn, Irstead. In: Murchison, C. (Ed.), Palaeontological Memoirs and Notes of Hugh Falconer, Vol. 2. Hardwicke, London, pp. 471–480.

Flerov, C.C., 1952. Musk Deer and Deer, in Fauna of the USSR: Mammals, Vols. 1-2. Israel Program for Scientific Translation, Jerusalem, 257 pp.

Fortelius, M., Eronen, J.T., Jernvall, J., Liu, L., Pushkina, D., Rinne, J., 2002. Fossil mammals resolve regional patterns of Eurasian climate change during 20 million years. Evolutionary Ecology Research 4, 1005–1016.

Frick, C., 1937. Horned ruminants of North America. Bulletin of the American Museum of Natural History 69, 1–669.

Gentry, A.W., 1994. The Miocene differentiation of Old World Pecora (Mammalia).

Historical Biology 7 (2), 115–158.

Goldfuss, G.A., 1820. Handbuch der Zoologie, Erste Abteilung. J.L. Schrag, Nürnberg, 696 pp.

Groves, C.P., Grubb, P., 1987. Relationships of living deer. In: Wemmer, C.M. (Ed.), Biology and Management of the Cervidae. Smithsonian Institute Press, Washington, pp. 21–59.

Groves, C., Grubb, P., 2011. Ungulate Taxonomy. The Johns Hopkins University Press, Baltimore, 309 pp.

Grubb, P., 2000. Valid and invalid nomenclature of living and fossil deer, Cervidae. Acta Theriologica 45 (3), 289–307.

Gustafson, E.P., 2015. An Early Pliocene North American deer: *Bretzia pseudalces*, its osteology, biology, and place in cervid history. Bulletin of the Museum of Natural History, University of Oregon 25, 1–75.

Han, D.F., 1987. Artiodactyla fossils from Liucheng *Gigantopithecus* Cave in Guangxi. Memoirs of Institute of Vertebrate Paleontology and Paleoanthropology, Academia Sinica 18, 135–208 (in Chinese, with English summary).

Heckeberg, N.S., 2017. A comprehensive approach towards the phylogeny and evolution of Cervidae. Doctoral Dissertation, Ludwig-Maximilians-Universität München, Facaulty of Geosciences, 424 pp.

Heintz, E., 1970. Les cervidés Villafranchiens de France et d'Espagne. Mémoires du Muséum National d'Histoire Naturelle, Nouvelle Série C, Sciences de la Terre 22, 1–303.

Huang, W.P., Li, Y., Nie, Z.S., 1989. Two new species of fossil *Megaceros* from North China. Vertebrata PalAsiatica 27 (1), 53–64 (in Chinese, with English abstract).

Ji, H.X., 1988. On the mandible thickness of *Megaceros* in China. Vertebrata PalAsiatica 26 (4), 296–302 (in Chinese, with English summary).

Kahlke, H.D., 1958. On the evolution of pachyostosis in jaw-bones of Choukoutien giant-deer *Megaceros pachyosteus* (Young). Vertebrata PalAsiatica 2 (2–3), 117–130.

Kahlke, H.D., 1997. Die Cerviden-Reste aus dem Untepleistozän von Untermassfeld. In: Kahlke, R.D. (Ed.), Das Pleistozän von Untermassfeld bei Meiningen (Thüringen). Dr Rudolf Habelt GMBH, Bonn, pp. 181–275.

Kierdorf, U., Flohr, S., Gomez, S., Landete-Castillejos, T., Kierdorf, H., 2013. The

structure of pedicle and hard antler bone in the European roe deer (*Capreolus capreolus*): a light microscope and backscattered electron imaging study. Journal of Anatomy 223, 364–384.

Kolb, C., Scheyer, T.M., Lister, A.M., Azorit, C., de Vos, J., Schlingemann, M.A.J., Rössner, G.E., Monaghan, N.T., Sánchez-Villagra, M.R., 2015. Growth in fossil and extant deer and implications for body size and life history evolution. BMC Evolutionary Biology 15, 1–15.

Leslie, D.M., 2011. *Rusa unicolor* (Artiodactyla: Cervidae). Mammalian Species 43 (1), 1–30.

Lin, Y.P., Pan, Y.R., Lu, Q.W., 1978. Early Pleistocene mammalian fauna from Yuanmou in Yunnan. In: Institute of Vertebrate Paleontology and Paleoanthropology, Academia Sinica (Ed.), Collected Papers of Paleoanthropology. Science Press, Beijing, pp. 101–125 (in Chinese).

Linnaeus, C., 1758. Systema naturae per regna tria naturae, secundum classes, ordines, genera, species, cum characteribus, differentiis, synonymis, locis. Volume 1: Regnum animale. Editio decima, reformata. Laurentii Salvii, Stockholm, 824 pp.

Lister, A.M., 1994. The evolution of the giant deer, *Megaloceros giganteus* (Blumenbach). Zoological Journal of the Linnean Society 112, 65–100.

Lister, A.M., 1996. The morphological distinction between bones and teeth of fallow deer (*Dama dama*) and red deer (*Cervus elaphus*). International Journal of Osteoarchaeology 6, 119–143.

Lister, A.M., Edwards, C.J., Nock, D.A.W., Bunce, M., van Pijlen, I.A., Bradley, D.G., Thomas, M.G., Barnes, I., 2005. The phylogenetic position of the 'giant deer' *Megaloceros giganteus*. Nature 438, 850–853.

Liu, P., Deng, C.L., Li, S.H., Cai, S.H., Cheng, H.J., Yuan, B.Y., Wei, Q., Zhu, R.X., 2012. Magnetostratigraphic dating of the Xiashagou Fauna and implication for sequencing the mammalian faunas in the Nihewan Basin, North China. Palaeogeography, Palaeoclimatology, Palaeoecology 315–316, 75–85.

Liu, P., Wu, Z., Deng, C., Tong, H.W., Qin, H.F., Li, S.H., Yuan, B.Y., Zhu, R.X., 2016. Magnetostratigraphic dating of the Shanshenmiaozui mammalian fauna in the Nihewan Basin, North China. Quaternary International 400, 202–211.

Lydekker, R., 1898. The Deer of All Lands: A History of the Family Cervidae, Living and Extinct. Rowland Ward Limited, London, 329 pp.

Madurell-Malapeira, J., Ros-Montoya, S., Espigares, M.P., Alba, D.M.,

Aurell-Garrido, J., 2014. Villafranchian large mammals from the Iberian Peninsula: paleogeography, paleoecology and dispersal events. Journal of Iberian Geology 40 (1), 167–178.

Martini, P., Geraads, D., 2018. *Camelus thomasi* Pomel, 1893, from the Pleistocene type-locality Tighennif (Algeria): Comparisons with modern *Camelus*. Geodiversitas 40 (5), 115–134.

Masini, F., Sala, B., 2007. Large- and small-mammal distribution patterns and chronostratigraphic boundaries from the Late Pliocene to the Middle Pleistocene of the Italian peninsula. Quaternary International 160, 43–56.

Meijaard, E., Groves, C., 2004. Morphometrical relationships between Southeast Asian deer (Cervidae, tribe Cervini): Evolutionary and biogeographic implications. Journal of Zoology 263, 179–196.

Mennecart, B., Demiguel, D., Bibi, F., Rössner, G.E., Metais, G., Neenan, J.M., Wang, S., Schulz, G., Muller, B., Costeur, L., 2017. Bony labyrinth morphology clarifies the origin and evolution of deer. Scientific Reports 7, Article number 13176, doi: 10.1038/s41598-017-12848-9.

Milne-Edwards, A., 1866. Note sur l'*Elaphurus davidianus*, espèce nouvelle de la famille des cerfs. Nouvelles Archives du Muséum d'Histoire Naturelle de Paris 2, 27–39.

Min, L.R., Chi, Z.Q., Wang, Y., Dong, J., Wang, Y.L., Zhu, G.X., 2015. Lithostratigraphic division and correlation of Haojiatai NHA borehole from Nihewan Basin in Yangyuan, Hebei. Geology in China 42 (4), 1068–1078 (in Chinese, with English abstract).

Morris, B., Mead, A.J., 2016. Body mass estimates from bone and tooth measurements in white-tailed deer, *Odocoileus virginianus*. Georgia Journal of Science 74 (2), Article 18, 1–6, https://digitalcommons.gaacademy.org/gjs/vol74/iss2/18/.

Nesti, F., 1841. Report of the meeting of Sept. 25th, summarized by Savi, P. and Sismonda A. Sezione di Geologia, Mineralogia, e Geografia, Atti della Terza Riunione degli Scienziati Italiani, Tenuta a Firenze 9 (6), 159.

Ohtaishi, N., 1992. White-lipped deer or Thorold's deer *Cervus albirostris*. In: Sheng, H.L. (Ed.), The Deer in China. East China Normal University Press, Shanghai, pp. 191–201 (in Chinese, with English summary).

O'Leary, M.A., Gatesy, J., 2008. Impact of increased character sampling on the

phylogeny of Cetartiodactyla (Mammalia): combined analysis including fossils. Cladistics 24, 397–442.

Otsuka, H., 1972. *Elaphurus shikamai* Otsuka (Pleistocene cervid) from the Akashi Formation of the Osaka Group, Japan, with special reference to the genus *Elaphurus*. Bulletin of the National Science Museum 15 (1), 197–210.

Owen, R., 1848. The Archetype and Homologies of the Vertebrate Skeleton. J. van Voorst, London, 203 pp.

Palmqvist, P., Gröcke, D.R., Arribas, A., Fariña, R.A., 2003. Paleoecological reconstruction of a lower Pleistocene large mammal community using biogeochemical ($\delta^{13}C$, $\delta^{15}N$, $\delta^{18}O$, Sr:Zn) and ecomorphological approaches. Paleobiology 29 (2), 205–229.

Pei, W.C., 1939. New fossil material and artifacts collected from the Choukoutien region during the years 1937 to 1939. Bulletin of the Geological Society of China 19 (3), 207–234.

Petronio, C., Krakhmalnaya, T., Belucci, L., Di Stefano, G., 2007. Remarks on some Eurasian pliocervines: Characteristics, evolution, and relationships with the tribe Cervini. Geobios 40, 113–130.

Pfeiffer, T., 2002. The first complete skeleton of *Megaloceros verticornis* (Dawkins, 1868) Cervidae, Mammalia, from Bilshausen (Lower Saxony, Germany): description and phylogenetic implications. Mitteilungen aus dem Museum für Naturkunde in Berlin, Geowiss Reihe 5, 289–308.

Pitra, C., Fickel, J., Meijaard, E., Groves, P.C., 2004. Evolution and phylogeny of old world deer. Molecular Phylogenetics and Evolution 33, 880–895.

Prummel, W., 1988. Distinguishing features on postcranial skeletal elements of cattle, *Bos primigenius* f. *taurus*, and red deer, *Cervus elaphus*. Schriften aus der Archäologisch-Zoologischen Arbeitsgruppe Schleswig-Kiel, Heft 12, 1–52.

Pueyo, E.L., Muñoz, A., Laplana, C., Parés, J.M., 2016. The Last Appearance Datum of *Hipparion* in Western Europe: magnetostratigraphy along the Pliocene–Pleistocene boundary in the Villarroya Basin (Northern Spain). International Journal of Earth Sciences 105 (8), 2203–2220.

Purdue, J.R., 1987. Estimation of body weight of white-tailed deer (*Odocoileus virginianus*) from bone size. Journal of Ethnobiology 7, 1–12.

Putman, R., 1988. The Natural History of Deer. Cornell University Press, New York, 191 pp.

Qiu, Z.X., 2000. Nihewan fauna and Q/N boundary in China. Quaternary Sciences 20 (2), 154–163 (in Chinese, with English abstract).

Qiu, Z.X., 2006. Quaternary environmental changes and evolution of large mammals in North China. Vertebrata PalAsiatica 44 (2), 109–132.

Qiu, Z.X., Deng, T., Wang, B.Y., 2004. Early Pleistocene mammalian fauna from Longdan, Dongxiang, Gansu, China. Palaeontologia Sinica, New Series C 27, 1–198 (in Chinese, with English summary).

Qiu, Z.X., Qiu, Z.D., Deng, T., Li, C.K., Zhang, Z.Q., Wang, B.Y., Wang, X.M., 2013. Neogene land mammal stages/Ages of China. In: Wang, X.M., Flynn, L.J., Fortelius, M. (Eds.), Fossil Mammals of Asia: Neogene Biostratigraphy and Chronology. Columbia University Press, New York, pp. 29–90.

Schmidt, K.T., Stien, A., Albon, S.D., Guinness, F.E., 2001. Antler length of yearling red deer is determined by population density, weather and early life-history. Oecologia 127, 191–197.

Scopoli, I.A., 1777. Introductio ad historiam naturalem sistens genera lapidum, plantarum, et animalium hactenus detecta, caracteribus essentialibus donata, in tribus divisa, subinde ad leges naturae. Apud Wolfgangum Gerle, Pragae, 540 pp.

Scott, K.M., 1983. Prediction of body weight of fossil Artiodactyla. Zoological Journal of the Linnean Society 77, 199–215.

Scott, K.M., 1990. Postcranial dimensions of ungulates as predictors of body mass. In: Damuth, J., Macfadden, B.J. (Eds.), Body Size in Mammalian Paleobiology: Estimation and Biological Implications. Cambridge University Press, Cambridge, pp. 301–336.

Senter, P., Moch, J.G., 2015. A critical survey of vestigial structures in the postcranial skeletons of extant mammals. Peer J 3, e1439, doi: 10.7717/peerj.1439.

Sheng, H.L. (Ed.), 1992. The Deer in China. East China Normal University Press, Shanghai, 305 pp. (in Chinese, with English summary).

Shikama, T., 1941. Fossil deer in Japan. In: Professor Yabe Sixtieth Birthday Commemoration Association (Ed.), Jubilee Publication in the Commemoration of Prof. H. Yabe's 60th Birthday, Vol. 2. Sasaki Printing Co., Tokyo, pp. 1125–1170.

Shpansky, A.V., 2014. Skeleton of the giant deer *Megaloceros giganteus giganteus* (Blumenbach, 1803) (Mammalia, Artiodactyla) from the Irtysh Region near

Pavlodar. Paleontological Journal 48 (5), 534–550.

Suraprasit, K., Jaeger, J.J., Chaimanee, Y., Chavasseau, O., Yamee, C., Tian, P., Panha, S., 2016. The Middle Pleistocene vertebrate fauna from Khok Sung (Nakhon Ratchasima, Thailand): biochronological and paleobiogeographical implications. Zookeys 613, 1–157.

Tang, Y.J., 1980. Early Pleistocene stratigraphy and mammalian fossils from Wenxi, Southwestern Shansi. Vertebrata PalAsiatica 18 (1), 33–44 (in Chinese, with English abstract).

Tang, Y.J., Zong, G.F., Xu, Q.Q., 1983. Mammalian fossils and stratigraphy of Linyi, Shansi. Vertebrata PalAsiatica 21 (1), 77–86 (in Chinese, with English abstract).

Tedford, R.N., Flynn, L.J., Qiu, Z.X., Opdyke, N.D., Downs, W.R., 1991. Yushe Basin, China: paleomagnetically calibrated mammalian biostratigraphic standard for the Late Neogene of Eastern Asia. Journal of Vertebrate Paleontology 11 (4), 519–526.

Teilhard de Chardin, P., 1936. Fossil mammals from locality 9 of Choukoutien. Palaeontologia Sinica, Series C 7 (4), 1–106.

Teilhard de Chardin, P., Leroy, P., 1942. Chinese fossil mammals. A complete bibliography, analyzed, tabulated, annotated and indexed. Institut de Géo-Biologie 8, 1–142.

Teilhard de Chardin, P., Piveteau, J., 1930. Les mammifères fossiles de Nihowan (Chine). Annales de Paleontologie 19, 1–134.

Teilhard de Chardin, P., Trassaert, M., 1937. Pliocene Camelidae, Giraffidae and Cervidae of south-eastern Shansi. Palaeontologia Sinica, New Series C 1, 1–68.

Teilhard de Chardin, P., Young, C.C., 1936. On the mammalian remains from the archaeological site of Anvang. Palaeontologica Sinica, Series C (1), 1–61.

Tong, H.W., 2012. New remains of *Mammuthus trogontherii* from the Early Pleistocene Nihewan beds at Shanshenmiaozui, Hebei. Quaternary International 255, 217–230.

Tong, H.W., Chen, X., 2015. On newborn calf skulls of Early Pleistocene *Mammuthus trogontherii* from Shanshenmiaozui in Nihewan Basin, China. Quaternary International 406, 57–69.

Tong, H.W., Wang, X.M., 2014. Juvenile skulls and other postcranial bones of *Coelodonta nihowanensis* from Shanshenmiaozui, Nihewan Basin, China. Journal of Vertebrate Paleontology 34 (3), 710–724.

Tong, H.W., Hu, N., Han, F., 2011. A preliminary report on the excavations at the Early Pleistocene fossil site of Shanshenmiaozui in Nihewan Basin, Hebei, China. Quaternary Sciences 31, 643–653 (in Chinese, with English abstract).

Tong, H.W., Chen, X., Zhang, B., 2017. New fossils of *Bison palaeosinensis* (Artiodactyla, Mammalia) from the steppe mammoth site of Early Pleistocene in Nihewan Basin, China. Quaternary International 445, 250–268.

Tong, Y.S., Zheng, S.H., Qiu, Z.D., 1995. Cenozoic mammal ages of China. Vertebrata PalAsiatica 33 (4), 290–314 (in Chinese, with English summary).

Trouessart, E.L., 1898-1899. Catalogus Mammalium tam viventium quam fossilium (nouvelle édit). R. Friedlander u. Sohn, Berlin, 1469 pp.

Valli, A.M.F., 2001. Le gisement Villafranchien Moyen de Saint-Vallier (Drôme): Nouvelles données paléontologiques (Cervidae, Bovinae) et taphonomiques. Documents des Laboratoires de Geologie Lyon 153, 1–275.

Valli, A.M.F., Palombo, M.R., 2005. Le régime alimentaire du Cervidae (Mammalia) *Eucladoceros ctenoides* (NESTI, 1841) reconstitué par la morphologie du crâne et par l'usure dentaire. Eclogae Geologicae Helvetiae 98, 133–143.

van der Made, J., 2015. The latest Early Pleistocene giant deer *Megaloceros novocarthaginiensis* n. sp. and the fallow deer *Dama* cf. *vallonnetensis* from Cueva Victoria (Murcia, Spain). Mastia 11–13, 269–323.

van der Made, J., in press. The dwarfed "giant deer" *Megaloceros matritensis* n. sp. from the Middle Pleistocene of Madrid — A descendant of *M. savini* and contemporary to *M. giganteus*. Quaternary International, doi: 10.1016/j.quaint.2018.06.006.

van der Made, J., Dimitrijević, V., 2015. *Eucladoceros montenegrensis* n. sp. and other Cervidae from the Lower Pleistocene of Trlica (Montenegro). Quaternary International 389, 90–118.

van der Made, J., Tong, H.W., 2008. Phylogeny of the giant deer with palmate brow tines *Megaloceros* from west and *Sinomegaceros* from east Eurasia. Quaternary International 179, 135–162.

Vislobokova, I.A., 1990. Fossil deer of Eurasia. Transactions of the Paleontological Institute 240, 1–206 (in Russian).

Vislobokova, I.A., 2008a. The major stages in the evolution of artiodactyl communities from the Pliocene–Early Middle Pleistocene of Northern Eurasia. Paleontological Journal 42 (3), 297–312.

Vislobokova, I.A., 2008b. Main stages in evolution of Artiodactyla communities from the Pliocene–Early Middle Pleistocene of Northern Eurasia: Part 2. Paleontological Journal 42 (4), 414–424.

Vislobokova, I.A., 2009. A new species of Megacerini (Cervidae, Artiodactyla) from the Late Miocene of Taralyk-Cher, Tuva (Russia), and remarks on the relationships of the group. Geobios 42, 397–410.

Vislobokova, I.A., 2012. Giant deer: origin, evolution, role in the biosphere. Paleontological Journal 46 (7), 643–775.

Vislobokova, I.A., 2013. Morphology, taxonomy, and phylogeny of Megacerines (Megacerini, Cervidae, Artiodactyla). Paleontological Journal 47 (8), 833–950.

Vislobokova, I.A., Hu, C., 1990. On the evolution of Megacerines, Vertebrata. PalAsiatica 28 (2), 150–158.

von den Driesch, A., 1976. A guide to the measurement of animal bones from archaeological sites. Peabody Museum Bulletin 1, 1–137.

Vukičević, T.T., Alic, I., Slavica, A., Poletto, M., Kužir, S., 2012. Preliminary osteometrical analysis of metapodium and acropodium bones of fallow deer (*Dama dama* L.) from the Brijuni Islands, Croatia. Veterinarski Arhiv 82 (1), 75–88.

Wang, H., 1988. An early Pleistocene mammalian fauna from Dali, Shaanxi. Vertebrata PalAsiatica 26 (1), 59–72 (in Chinese, with English abstract).

Wang, L.H., Zhang, Z.Q., 2014. Late Miocene *Cervavitus novorossiae* (Cervidae, Artiodactyla) from Lantian, Shaanxi Province. Vertebrata PalAsiatica 52 (3), 303–315.

Wemmer, C., 1983. Systematic position and anatomical traits. In: Beck, B. (Ed.), The Biology and Management of An Extinct Species — Pere David's Deer. Noyes Publications, Park Ridge, New Jersey, pp. 15–20.

Woodburne, M.O., Tedford, R.H., Lindsay, E., 2013. North China Neogene Biochronology: A Chinese standard. In: Wang, X.M., Flynn, L.J., Fortelius, M. (Eds.), Fossil Mammals of Asia: Neogene Biostratigraphy and Chronology. Columbia University Press, New York, pp. 91–123.

Wu, J.Y., Wang, W., 1999. The White-lipped Deer of China. China Forestry Publishing House, Beijing, 167 pp. (in Chinese, with English abstract).

Young, C.C., 1932. On the artiodactyla from the *Sianthropus* site at Choukoutien. Palaeontologia Sinica, Series C 8 (2), 1–100.

Young, C.C., 1935. Miscellaneous mammalian fossils from Shansi and Honan. Palaeontologia Sinica, Series C 9 (2), 1–56.

Zdansky, O., 1925. Fossile Hirsche Chinas. Palaeontologia Sinica, Series C 2 (3), 1–90.

Zdansky, O., 1927. Weitere Bemerkungen über fossile Cerviden aus China. Palaeontologia Sinica, Series C 5 (1), 1–19.

Zhang, B., Chen, X., Tong, H.W., 2018. Tooth remains of Late Pleistocene moschid and cervid (Artiodactyla, mammalia) from Yangjiawan and Fuyan Caves of southern China. Quaternary International 490, 21–32.

Zheng, S.H., Han, D.F., 1993. Mammalian fossils. In: Zhang, S.S. (Ed.), Comprehensive Study on the Jinniushan Paleolithic Site. Memoirs of Institute of Vertebrate Paleontology and Paleoanthropology, Academia Sinica 19, 43–127 (in Chinese, with English summary).

Zheng, S.H., Wu, W.Y., Li, Y., Wang, G.D., 1985. Late Cenozoic mammalian faunas of Guide and Gonghe Basin, Qinghai Province. Vertebrata PalAsiatica 23 (2), 89–134 (in Chinese, with English summary).

Zhu, R.X., Hoffman, K.A., Potts, R., Deng, C.L., Pan, Y.X., Guo, B., Shi, C.D., Guo, Z.T., Yuan, B.Y., Hou, Y.M., Huang, W.W., 2001. Earliest presence of humans in Northeast Asia. Nature 413, 413–417.

Zhu, R.X., Deng, C.L., Pan, Y.X., 2007. Magnetochronology of the fluvio-lacustrine sequences in the Nihewan Basin and its implications for Early Human colonization of Northeast Asia. Quaternary Sciences 27 (6), 922–944 (in Chinese, with English abstract).

Zhu, Z.Y., Dennell, R., Huang, W.W., Wu, Y., Rao, Z.G., Qiu, S.F., Xie, J.B., Liu, W., Fu, S.Q., Han, J.W., Zhou, H.Y., Ou Yang, T.P., Li, H.M., 2015. New dating of the *Homo erectus* cranium from Lantian (Gongwangling), China. Journal of Human Evolution 78, 144–157.

Fig. 1. Map of fossil localities and chronology of *E. boulei* in northern China.

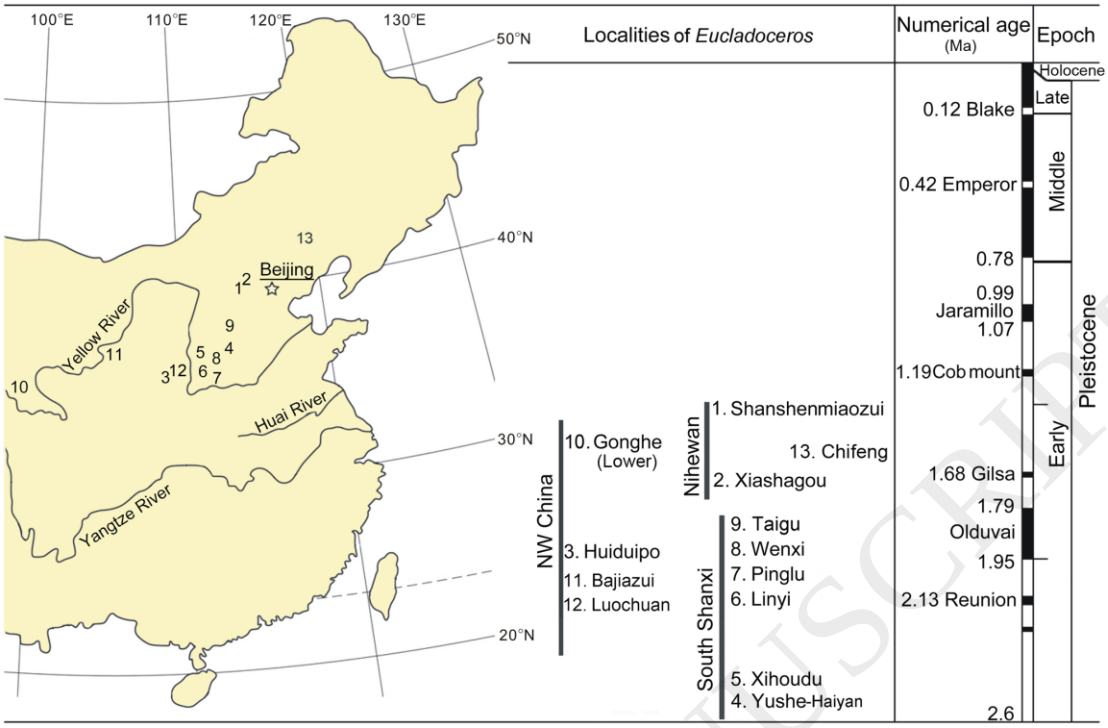

Fig. 2. Dental terminology. (A) Left DP2; (B) left DP3; (C) left DP4; (D) right M2-3; (E) right dp2; (F) right dp3; (G) right dp4; (H) right m2-3; (I) right m1-2. (A-C, E-G) Occlusal views; (D, I), buccal views; (H) lingual view.

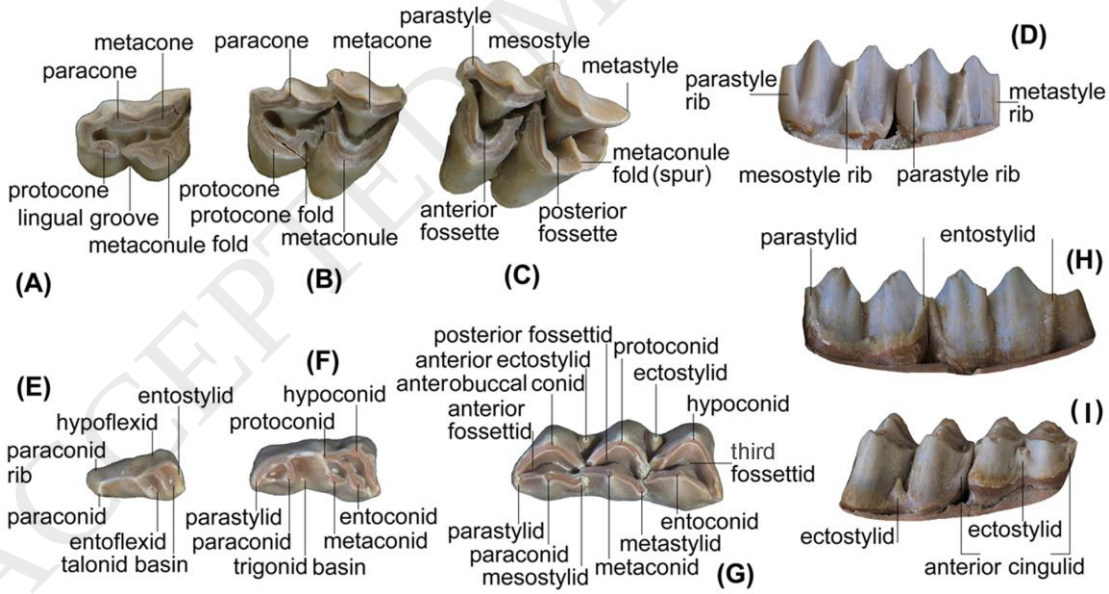

Fig. 3. Yearling antler (or spike) of *E. boulei* from SSMZ, in anterior view. (A) Right antler (IVPP V 25966.2); (B) left antler (IVPP V 25966.1); (C) image of CT scanning, showing the boundary between the antler and the pedicle (indicated by arrows).

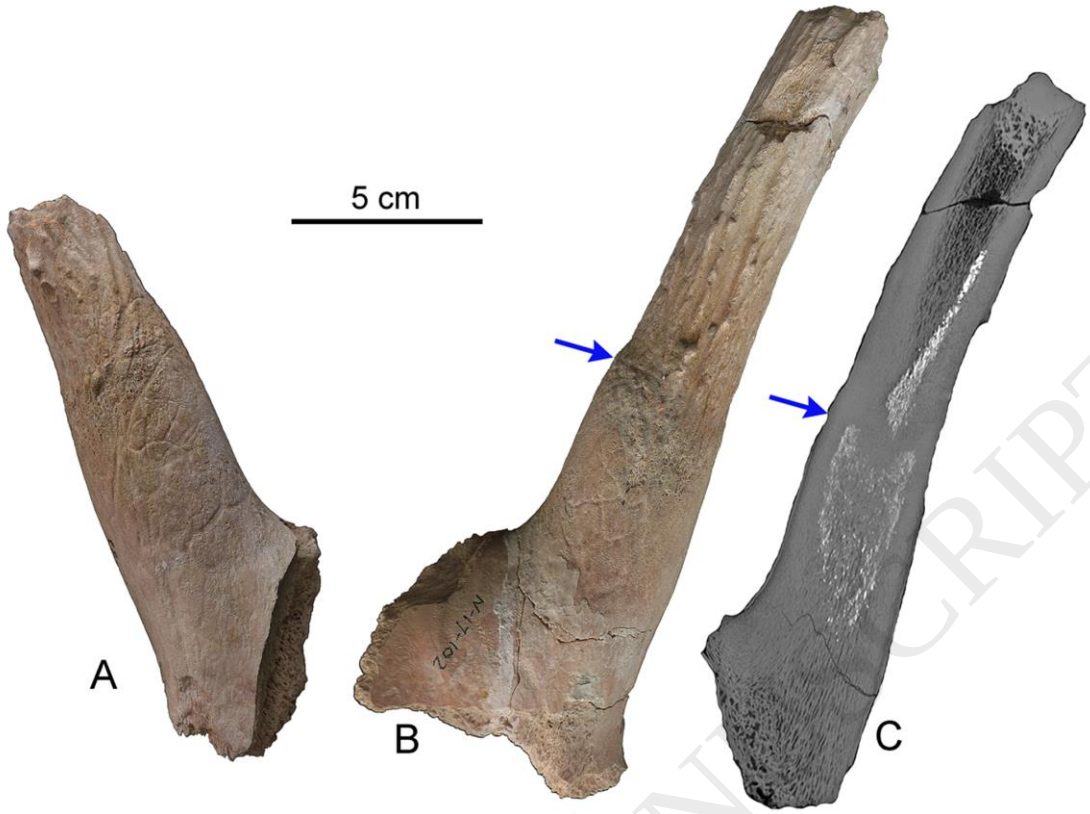

Fig. 4. Maxilla and mandibles with deciduous teeth of *E. boulei* from SSMZ. (A1-A3) IVPP V 25966.3, maxilla with DP2-4. (B1-B3) IVPP V 25966.5, right mandible with dp2-4. (C1-C3) IVPP V 25966.4; (C1, C2) left mandible with dp2-m1; (C3) details of dp2-4. (A1, B1, C1) Buccal views; (A2, B2) lingual views; (A3, B3, C2, C3) occlusal views. Scale bar = 5 cm.

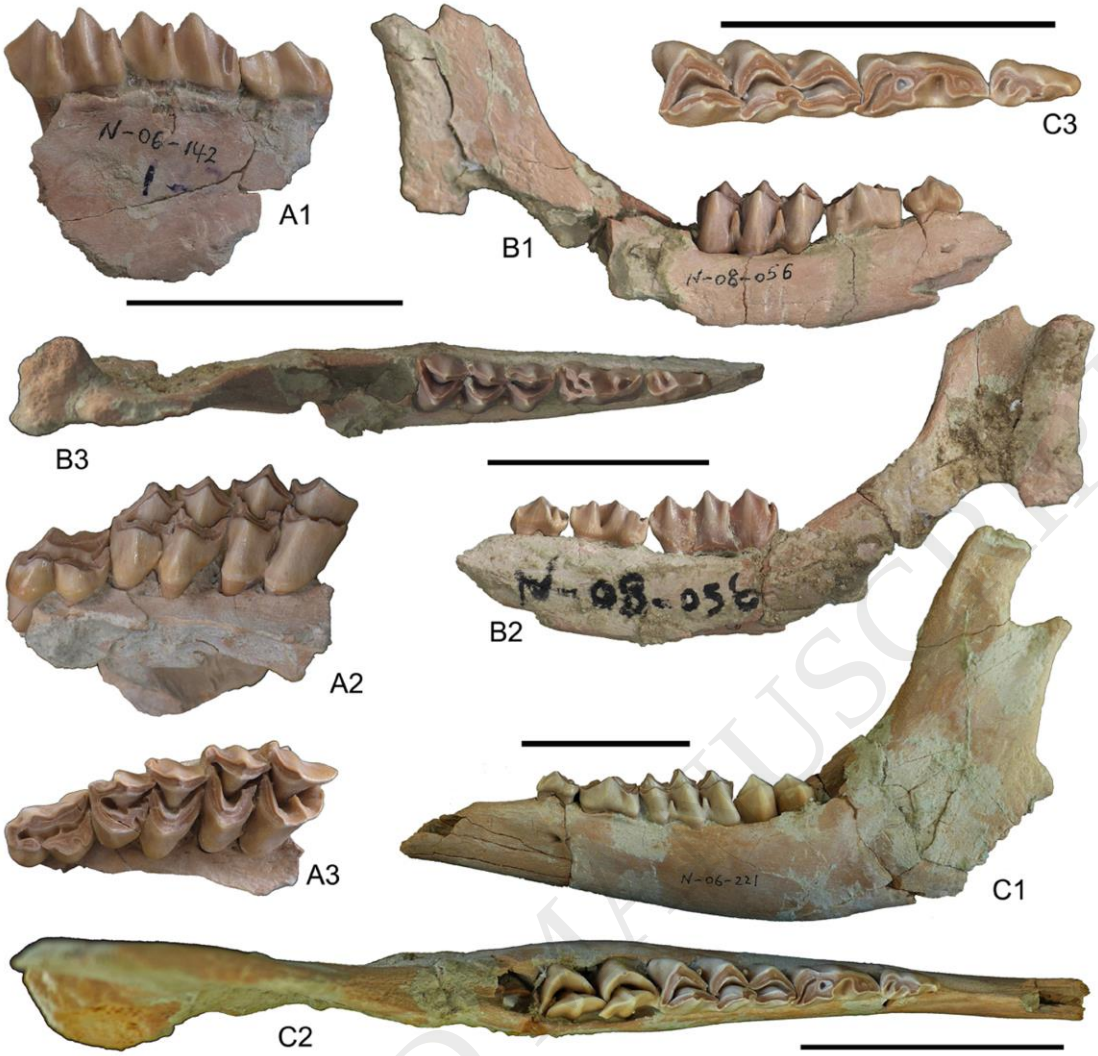

Fig. 5. Maxillae with permanent teeth of *E. boulei* from SSMZ. (A1, A2) IVPP V 25966.17, left maxilla with P4-M3. (B1-B3) IVPP V 25966.18, right maxilla with P2-M2. (C1-C3) IVPP V 25966.14, right maxilla with P3-M3. (A1, B1, C1) Lingual views; (A2, B2, C2) occlusal views; (B3, C3) buccal view. Scale bar = 5 cm.

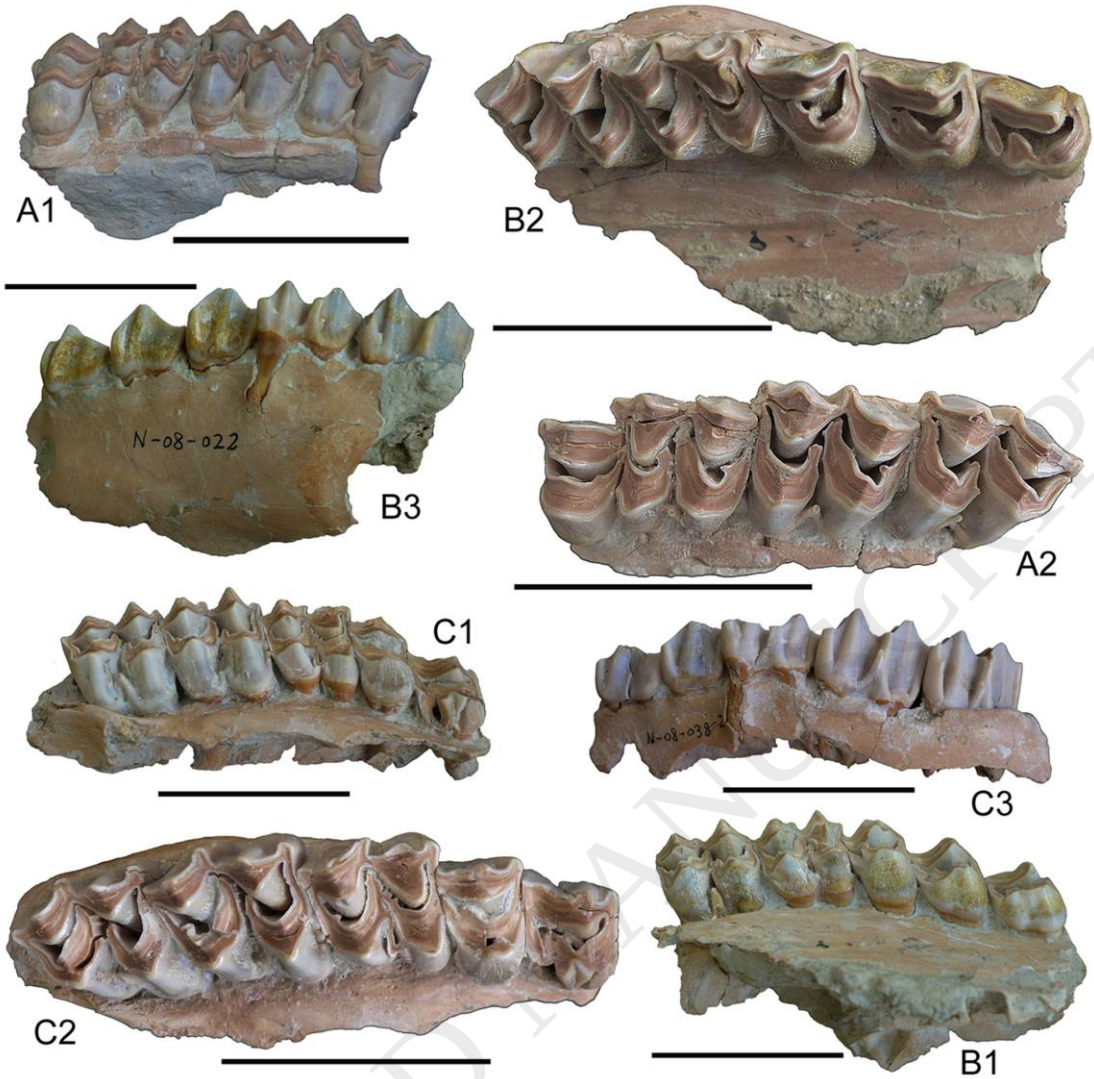

Fig. 6. Mandibles with permanent teeth of *E. boulei* from SSMZ. (A1, A2) IVPP V 25966.24, right mandible with i1-3, c and p2-m3. (B1-B5) IVPP V 25966.15, right mandible with p3-m3. (C1-C4) IVPP V 25966.16; (C1-C3) left mandible with p2-m3; (C4) details of p2-m3. (A1, B1, C1) Buccal views; (B2, C2) lingual views; (A2, B3, C3, C4) occlusal views; (B4) CT scanning images in front of m2; (B5) CT scanning images in front of m3. Scale bar = 5 cm.

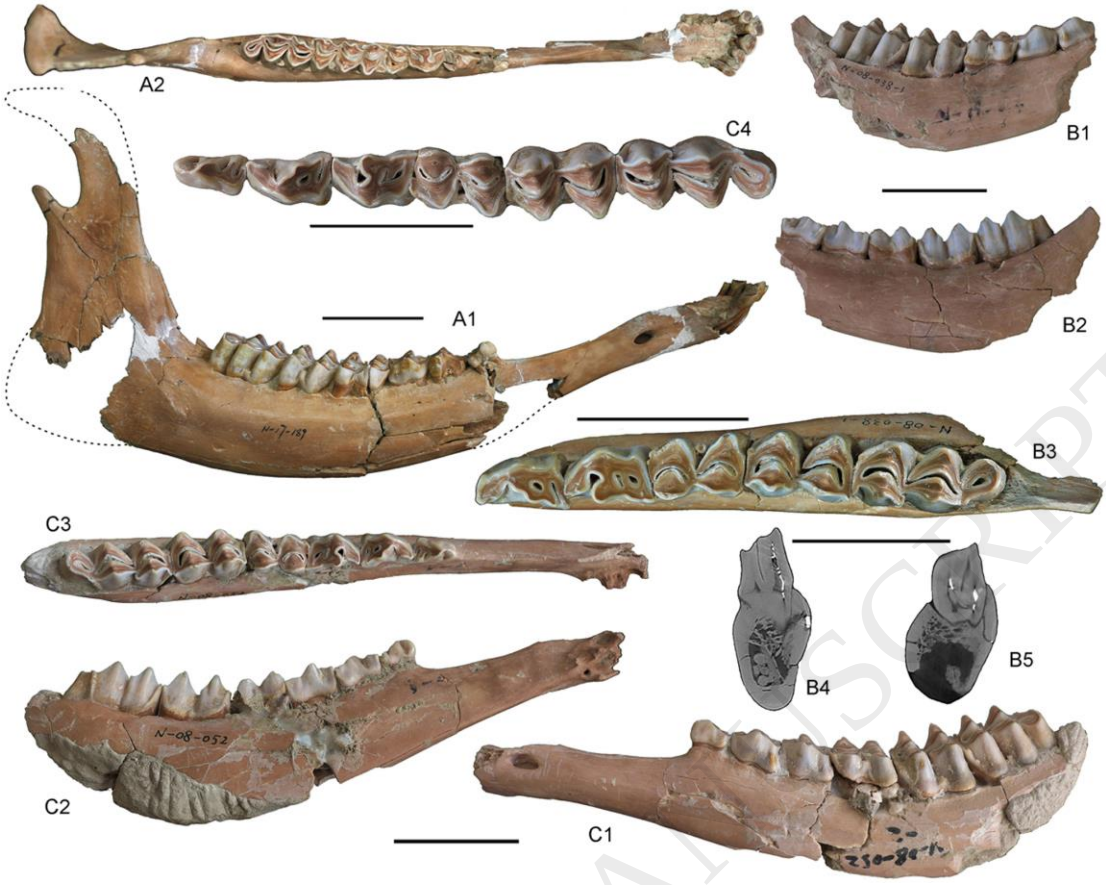

Fig. 7. Postcranial bones other than metapodials of *E. boulei* from SSMZ. (A1, A2) IVPP V 25966.25, right scapula. (B) IVPP V 25966.26 + IVPP V 25966.27, articulated right humerus and radius as well as ulna. (C1-C4) IVPP V 25966.27, right radius-ulna. (D1-D3) IVPP V 25966.26, distal part of right humerus. (E1-E3) IVPP V 25966.36, distal part of right tibia. (F1-F4) IVPP V 25966.46, left calcaneum. (G1, G2) IVPP V 25966.40, right astragalus. (H1, H2) IVPP V 25966.42, left naviculo-cuboid (centrotarsale). (A1, C2, F1) Lateral views; (A2, C4, D3, E3, H2) distal views; (B, C3, F2) medial views; (C1, D1, E2, F3, G1) anterior views; (D2, E1, F4, G2) posterior views; (H1) proximal view. Scale bar = 10 cm; (C4, E3, G1, G2, H1, H2) are englarged by two times.

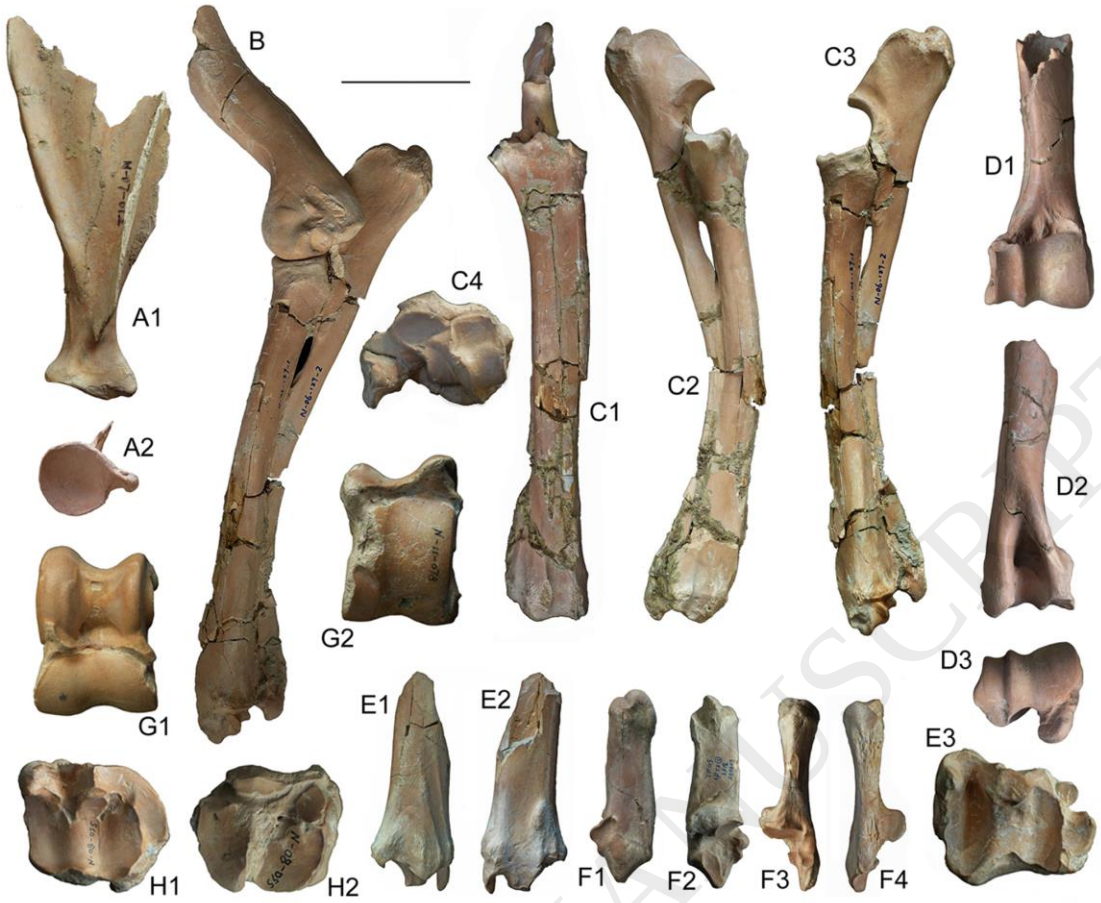

Fig. 8. Metapodials of *E. boulei* from SSMZ (A-E), compared with that of fossil *C. nippon* from Tianyuandong (F). (A1-A4) IVPP V 25966.28, left Mc III+4. (B1-B4) IVPP V 25966.39, left Mc III+4. (C1, C2) IVPP V 25966.44, left Mt III+IV. (D1-D3) IVPP V 25966.45, right Mt III+IV. (E1-E3) IVPP V 25966.29, left Mt III+IV. (F) IVPP V 13729.8, right Mt III+IV. (A1, B1, C1, D1, E1, F) Anterior views; (A2, A4, B2, C2, D2, E2) posterior views; (A3, B3, E3) proximal views; (B4, D3) distal views. Scale bar = 10 cm; (A3, A4, A5, B3, B4, E3) are englarged by two times.

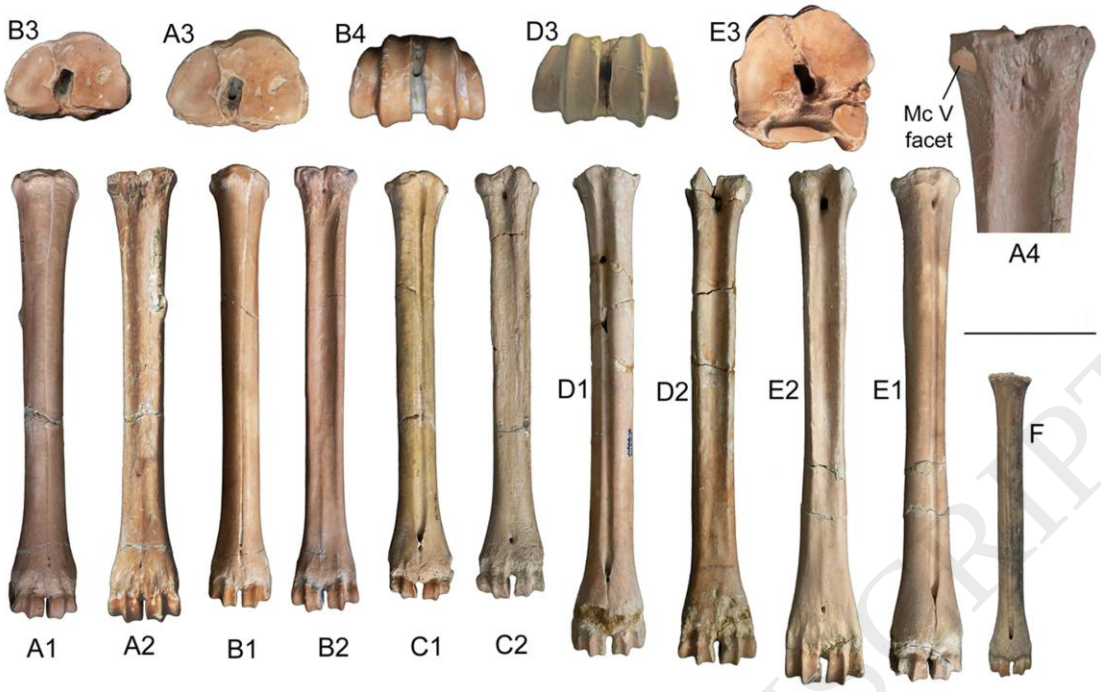

Fig. 9. Relationships between body weight and metapodial dimensions as well as lower toothrow length.

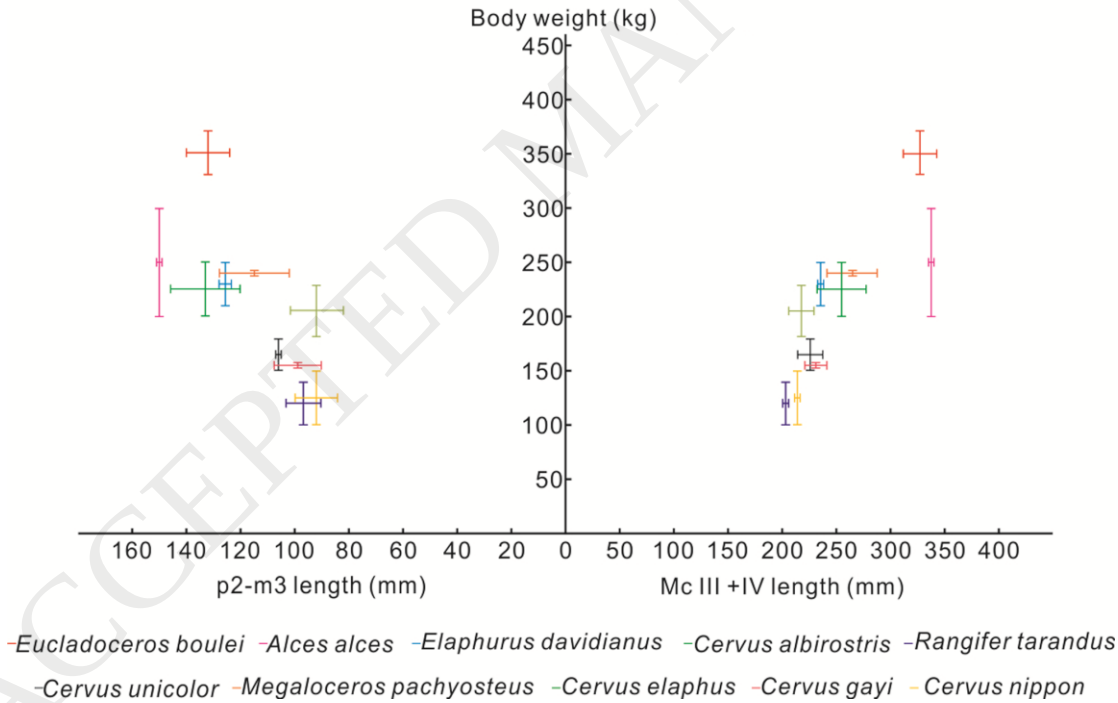

Fig. 10. Temporal distribution of Villafranchian and later cervids in northern China. All the bars represent the temporal arrangements of each taxon; each animal's icon size approximately corresponds with its body weight on the weight scale at the right. The Neogene fossil records are after Tedford et al. (1991), Dong (1993) and Qiu et al. (2013).